Low-complexity 8-point DCT Approximation Based on Angle Similarity for Image and Video Coding

Raíza S. Oliveira [*] Renato J. Cintra [†] Fábio M. Bayer [‡] Thiago L. T. da Silveira [§] Arjuna Madanayake[¶]
André Leite [‖]

Abstract

The principal component analysis (PCA) is widely used for data decorrelation and dimensionality reduction. However, the use of PCA may be impractical in real-time applications, or in situations were energy and computing constraints are severe. In this context, the discrete cosine transform (DCT) becomes a low-cost alternative to data decorrelation. This paper presents a method to derive computationally efficient approximations to the DCT. The proposed method aims at the minimization of the angle between the rows of the exact DCT matrix and the rows of the approximated transformation matrix. The resulting transformations matrices are orthogonal and have extremely low arithmetic complexity. Considering popular performance measures, one of the proposed transformation matrices outperforms the best competitors in both matrix error and coding capabilities. Practical applications in image and video coding demonstrate the relevance of the proposed transformation. In fact, we show that the proposed approximate DCT can outperform the exact DCT for image encoding under certain compression ratios. The proposed transform and its direct competitors are also physically realized as digital prototype circuits using FPGA technology.

Keywords

DCT Approximation, Fast algorithms, Image/video encoding

1 Introduction

Data decorrelation is a central task in many statistical and signal processing problems [1–3]. Decorrelation can be accomplished by means of a linear transformation that converts correlated observations into linearly uncorrelated values. This operation is commonly performed by principal component analysis (PCA) [2]. PCA is widely used to reduce the dimensionality of data [2, 4], where the information contained in all the original variables is replaced by the data variability information of the initial few uncorrelated principal components. The quality of such approximation depends on the number of components used and the proportion of variance explained, or energy retained, by each of them.

In the field of analysis and processing of images and signals, PCA, also known as the discrete Karhunen–Loève transform (KLT) [3], is considered the optimal linear transformation for data decorrelation when the signal is a first order Markov process [3, 5]. The KLT has the following features [3]: (i) decorrelates the input data completely in the transform domain; (ii) minimizes the mean square error in data compression; and (iii) concentrates the energy (variance) in a few coefficients of the output vector. Because the KLT matrix depends on the variance and covariance matrix of the input data, deriving computationally efficient algorithms for real-time processing becomes a very hard task [3, 6–13].

If the input data follows a stationary highly correlated first-order Markov process [3, 12, 14], then the KLT is very closely approximated by the discrete cosine transform (DCT) [3, 12]. Natural images fall into this particular statistical model category [15]. Thus DCT inherits the decorrelation and compaction properties of the KLT, with the advantage of having a closed-form expression independent of the input signal. Image and video communities widely adopt the DCT in their most successful compression standards, such as JPEG [16] and MPEG [17]. Often such standards include two-dimensional (2-D) versions of the DCT applied to small image blocks ranging from 4×4 to 32×32 pixels.

The 8×8 block is employed in a large number of standards, for example: JPEG [16], MPEG [18], H.261 [19], H.263 [20], H.264/AVC [21], and HEVC [22]. The arithmetic cost of the 8-point DCT is 64 multiplications and 56 additions, when computed by definition. Fast algorithms can dramatically reduce the arithmetic cost to 11 multiplications and 29 additions, as in the Loeffler DCT algorithm [23].

However, the number of DCT calls in common image and video encoders is extraordinarily high. For instance, a single image frame of high-definition TV (HDTV) contains 32.400 8×8 image subblocks. Therefore, computational savings in the DCT step may effect significant performance gains, both in terms of speed and power consumption [24, 25]. Being quite a mature area of research [26], there is little room for improvement on the exact DCT computation. Thus, one approach to further minimize the computational cost of computing the DCT is the use of matrix approximations [14, 27]. Such approximations provide matrices with similar mathematical behavior to the exact DCT while presenting a dramatically low arithmetic cost.

The goals of this paper are as follows. First, we aim at establishing an optimization problem to facilitate the derivation of 8-point DCT approximations. To this end, we adopt a vector angle based objective function to minimize the angle between the rows of the approximate and the exact DCT matrices subject to orthogonality constraints. Second, the sought approximations are (i) submitted to a comprehensive assessment based on well-known figures of merit and (ii) compared to state-of-the-art DCT approximations. Third, fast algorithms are derived and realized in FPGA hardware with comparisons with competing methods. We also examine the performance of the obtained transformations in the context of image compression and video coding. We demonstrate that one of our DCT approximations can outperform the exact DCT in terms of effected quality after image compression.

This paper is organized as follows. In Section 2, the 8-point DCT and popular DCT approximations are discussed. Section 3 introduces an optimization problem to pave the way for the derivation of new DCT approximations. In Section 4 the proposed approximations are detailed

[*] R. S. Oliveira is with the Programa de Pós-Graduação em Engenharia Elétrica, Universidade Federal de Pernambuco (UFPE), Recife, Brazil; and with the Signal Processing Group, Departamento de Estatística, UFPE.

[†] Renato J. Cintra is with the Signal Processing Group, Departamento de Estatística, Universidade Federal de Pernambuco, Recife, Brazil; ECE, University of Calgary, Calgary, AB, Canada. E-mail: rjdsc@de.ufpe.br

[‡] F. M. Bayer is with the Departamento de Estatística, Universidade Federal de Santa Maria, Santa Maria, and LACESM, Brazil.

[§] T. L. T. Silveira is with the Programa de Pós-Graduação em Computação, Universidade Federal do Rio Grande do Sul, Porto Alegre, Brazil.

[¶] Arjuna Madanayake is with the Department of Electrical and Computer Engineering, University of Akron, Akron, OH.

[‖] André Leite is with the Departamento de Estatística, Universidade Federal de Pernambuco, Recife, Brazil. E-mail: leite@de.ufpe.br

Table 1: Computational cost of the fast algorithms for the DCT

Algorithm	Multiplications	Additions
Loeffler *et al.* [23,35,36]	11	29
Yuan *et al.* [28,37]	12	29
Lee [32,38,39]	12	29
Hou [33,40,41]	12	29
Arai *et al.* [29,35,42]	13	29
Chen *et al.* [30,35,43]	16	26
Feig–Winograd [31,44]	22	28

and assessed according to well-known performance measures. In Section 5 a fast algorithm for the proposed approximation is presented. Moreover, a field-programmable gate array (FPGA) design is proposed and compared with competing methods. Section 6 furnishes computational evidence of the appropriateness of the introduced approximate DCT for image and video encoding. Section 7 concludes the paper.

2 DCT Approximations

Let $\mathbf{x}$ and $\mathbf{X}$ be 8-point column vectors related by the DCT. Therefore, they satisfy the following expression: $\mathbf{X} = \mathbf{C} \cdot \mathbf{x}$, where

$$\mathbf{C} = \begin{bmatrix} \gamma_3 & \gamma_3 & \gamma_3 & \gamma_3 & \gamma_3 & \gamma_3 & \gamma_3 & \gamma_3 \\ \gamma_0 & \gamma_2 & \gamma_4 & \gamma_6 & -\gamma_6 & -\gamma_4 & -\gamma_2 & -\gamma_0 \\ \gamma_1 & \gamma_5 & -\gamma_5 & -\gamma_1 & -\gamma_1 & -\gamma_5 & \gamma_5 & \gamma_1 \\ \gamma_2 & -\gamma_6 & -\gamma_0 & -\gamma_4 & \gamma_4 & \gamma_0 & \gamma_6 & -\gamma_2 \\ \gamma_3 & -\gamma_3 & -\gamma_3 & \gamma_3 & \gamma_3 & -\gamma_3 & -\gamma_3 & \gamma_3 \\ \gamma_4 & -\gamma_0 & \gamma_6 & \gamma_2 & -\gamma_2 & -\gamma_6 & \gamma_0 & -\gamma_4 \\ \gamma_5 & -\gamma_1 & \gamma_1 & -\gamma_5 & -\gamma_5 & \gamma_1 & -\gamma_1 & \gamma_5 \\ \gamma_6 & -\gamma_4 & \gamma_2 & -\gamma_0 & \gamma_0 & -\gamma_2 & \gamma_4 & -\gamma_6 \end{bmatrix},$$

and $\gamma_k = \cos(2\pi(k+1)/32)$, for $k = 0, 1, \ldots, 6$.

Common algorithms for efficient DCT computation include: (i) Yuan *et al.* [28], (ii) Arai *et al.* [29], (iii) Chen *et al.* [30], (iv) Feig–Winograd [31], (v) Lee [32], and (vi) Hou [33]. Table 1 lists the computational costs associated to such methods. The theoretical minimal multiplicative complexity is 11 multiplications [23,34], which is attained by the Loeffler algorithm [23].

A DCT approximation is a matrix $\widehat{\mathbf{C}}$ capable of furnishing $\widehat{\mathbf{X}} = \widehat{\mathbf{C}} \cdot \mathbf{x}$ where $\widehat{\mathbf{X}} \approx \mathbf{X}$ according to some prescribed criterion, such as matrix proximity or coding performance [3]. In general terms, as shown in [3,45–48], $\widehat{\mathbf{C}}$ is a real valued matrix which consists of two components: (i) a low-complexity matrix $\mathbf{T}$ and (ii) a diagonal matrix $\mathbf{S}$. Such matrices are given by:

$$\widehat{\mathbf{C}} = \mathbf{S} \cdot \mathbf{T}, \tag{1}$$

where

$$\mathbf{S} = \sqrt{(\mathbf{T} \cdot \mathbf{T}^\top)^{-1}}. \tag{2}$$

The operation $\sqrt{\cdot}$ is the matrix square root operation [49,50].

Hereafter *low-complexity* matrices are referred to as $\mathbf{T}_*$, where the subscript $*$ indicates the considered method. Also *DCT approximations* are referred to as $\hat{\mathbf{C}}_*$. If the subscript is absent, then we refer to a generic low-complexity matrix or DCT approximation.

A traditional DCT approximation is the signed DCT (SDCT) [51] which matrix is obtained according to: $\frac{1}{\sqrt{8}} \cdot \operatorname{sgn}(\mathbf{C})$, where $\operatorname{sgn}(\cdot)$ is the entry-wise signum function. Therefore, in this case, the entries of the associated low-complexity matrix $\mathbf{T}_{\text{SDCT}} = \operatorname{sgn}(\mathbf{C})$ are in $\{0, \pm 1\}$. Thus matrix $\mathbf{T}_{\text{SDCT}}$ is multiplierless.

Notably, in the past few years, several approximations for the DCT have been proposed as, for example, the rounded DCT (RDCT, $\mathbf{T}_{\text{RDCT}}$) [27], the modified RDCT (MRDCT, $\mathbf{T}_{\text{MRDCT}}$) [48], the series of approximations proposed by Bouguezel–Ahmad–Swamy (BAS) [52–56], the Lengwehasatit–Ortega approximation (LO, $\mathbf{T}_{\text{LO}}$) [57], the approximation proposed by Pati *et al.* [58], and the collection of approximations introduced in [14]. Most of these approximations are orthogonal with low computational complexity matrix entries. Essentially, they are matrices defined over the set $\{0, \pm 1/2, \pm 1, \pm 2\}$, with the multiplication by powers of two implying simple bit-shifting operations.

Such approximations were demonstrated to be competitive substitutes for the DCT and its related integer transformations as shown in [14,27,48,52–57]. Table 2 illustrates some common integer transformations linked to the DCT approximations.

Table 2: Common 8-point low-complexity matrices associated to DCT approximations

Method	Transformation Matrix
$\mathbf{T}_{\text{RDCT}}$ [27]	$\begin{bmatrix} 1 & 1 & 1 & 1 & 1 & 1 & 1 & 1 \\ 1 & 1 & 1 & 0 & 0 & -1 & -1 & -1 \\ 1 & 0 & 0 & -1 & -1 & 0 & 0 & 1 \\ 1 & 0 & -1 & -1 & 1 & 1 & 0 & -1 \\ 1 & -1 & -1 & 1 & 1 & -1 & -1 & 1 \\ 1 & -1 & 0 & 1 & -1 & 0 & 1 & -1 \\ 0 & -1 & 1 & 0 & 0 & 1 & -1 & 0 \\ 0 & -1 & 1 & -1 & 1 & -1 & 1 & 0 \end{bmatrix}$
$\mathbf{T}_{\text{BAS-2008b}}$ [52]	$\begin{bmatrix} 1 & 1 & 1 & 1 & 1 & 1 & 1 & 1 \\ 1 & 1 & 1 & 0 & 0 & -1 & -1 & -1 \\ 1 & 1 & -1 & -1 & -1 & -1 & 1 & 1 \\ 1 & 0 & -1 & 0 & 0 & 1 & 0 & -1 \\ 1 & -1 & -1 & 1 & 1 & -1 & -1 & 1 \\ 1 & -1 & 1 & 0 & 0 & -1 & 1 & -1 \\ 1 & -1 & 1 & -1 & -1 & 1 & -1 & 1 \\ 1 & -1 & 1 & -1 & 1 & -1 & 1 & -1 \end{bmatrix}$
$\mathbf{T}_{\text{LO}}$ [57]	$\begin{bmatrix} 1 & 1 & 1 & 1 & 1 & 1 & 1 & 1 \\ 1 & 1 & 1 & 0 & 0 & -1 & -1 & -1 \\ 1 & \frac{1}{2} & -\frac{1}{2} & -1 & -1 & -\frac{1}{2} & \frac{1}{2} & 1 \\ 1 & 0 & -1 & -1 & 1 & 1 & 0 & -1 \\ 1 & -1 & -1 & 1 & 1 & -1 & -1 & 1 \\ 1 & -1 & 0 & 1 & -1 & 0 & 1 & -1 \\ \frac{1}{2} & -1 & 1 & -\frac{1}{2} & -\frac{1}{2} & 1 & -1 & \frac{1}{2} \\ 0 & -1 & 1 & -1 & 1 & -1 & 1 & 0 \end{bmatrix}$
$\mathbf{T}_6$ [14]	$\begin{bmatrix} 1 & 1 & 1 & 1 & 1 & 1 & 1 & 1 \\ 2 & 1 & 1 & 0 & 0 & -1 & -1 & -2 \\ 2 & 1 & -1 & -2 & -2 & -1 & 1 & 2 \\ 1 & 0 & -2 & -1 & 1 & 2 & 0 & -1 \\ 1 & -1 & -1 & 1 & 1 & -1 & -1 & 1 \\ 1 & -2 & 0 & 1 & -1 & 0 & 2 & -1 \\ 1 & -2 & 2 & -1 & -1 & 2 & -2 & 1 \\ 0 & -1 & 1 & -2 & 2 & -1 & 1 & 0 \end{bmatrix}$
$\mathbf{T}_4$ [14]	$\begin{bmatrix} 1 & 1 & 1 & 1 & 1 & 1 & 1 & 1 \\ 1 & 1 & 1 & 0 & 0 & -1 & -1 & -1 \\ 1 & 1 & -1 & -1 & -1 & -1 & 1 & 1 \\ 1 & 0 & -1 & -1 & 1 & 1 & 0 & -1 \\ 1 & -1 & -1 & 1 & 1 & -1 & -1 & 1 \\ 1 & -1 & 0 & 1 & -1 & 0 & 1 & -1 \\ 1 & -1 & 1 & -1 & -1 & 1 & -1 & 1 \\ 0 & -1 & 1 & -1 & 1 & -1 & 1 & 0 \end{bmatrix}$

3 Greedy Approximations

3.1 Optimization Approach

Approximate DCT matrices are often obtained by fully considering the exact DCT matrix $\mathbf{C}$, including its symmetries [59], fast algorithms [23,33], parametrizations [31], and numerical properties [28]. Usually the low-complexity component of a DCT approximation is found by solving the following optimization problem:

$$\mathbf{T} = \arg\min_{\mathbf{T}'} \operatorname{approx}(\mathbf{T}', \mathbf{C}),$$

where $\operatorname{approx}(\cdot, \cdot)$ is a particular approximation assessment function—such as proximity measures and coding performance metrics [3]—and subject to various constraints, such as orthogonality and low-complexity of the candidate matrices $\mathbf{T}'$.

However, the DCT matrix can be understood as a stack of row vectors $\mathbf{c}_k^\top$, $k = 1, 2, \ldots, 8$, as follows:

$$\mathbf{C} = \begin{bmatrix} \mathbf{c}_1 & \mathbf{c}_2 & \mathbf{c}_3 & \mathbf{c}_4 & \mathbf{c}_5 & \mathbf{c}_6 & \mathbf{c}_7 & \mathbf{c}_8 \end{bmatrix}^\top. \tag{3}$$

In the current work, to derive an approximation for $\mathbf{C}$, we propose to individually approximate each of its rows in the hope that the set of approximate rows generate a good approximate matrix. Such heuristic

Table 3: Examples of approximated vectors for the search space $\mathscr{D}_1$

n	Approximated Vector
1	$[1 \quad 1 \quad 1 \quad 1 \quad 1 \quad 1 \quad 1 \quad 1]^\top$
2	$[1 \quad 1 \quad 1 \quad 1 \quad 1 \quad 1 \quad 1 \quad -1]^\top$
3	$[1 \quad 1 \quad 1 \quad 1 \quad 1 \quad 1 \quad 1 \quad 0]^\top$
4	$[1 \quad 1 \quad 1 \quad 1 \quad 1 \quad 1 \quad -1 \quad 1]^\top$
$\vdots$	$\vdots$
6558	$[-1 \quad -1 \quad -1 \quad -1 \quad -1 \quad -1 \quad 1 \quad -1]^\top$
6559	$[-1 \quad -1 \quad -1 \quad -1 \quad -1 \quad -1 \quad -1 \quad 1]^\top$
6560	$[-1 \quad -1 \quad -1 \quad -1 \quad -1 \quad -1 \quad -1 \quad 0]^\top$
6561	$[-1 \quad -1 \quad -1 \quad -1 \quad -1 \quad -1 \quad -1 \quad -1]^\top$

Table 4: Examples of approximated vectors for the search space $\mathscr{D}_2$

n	Approximated Vector
1	$[2 \quad 2 \quad 2 \quad 2 \quad 2 \quad 2 \quad 2 \quad -1]^\top$
2	$[2 \quad 2 \quad 2 \quad 2 \quad 2 \quad 2 \quad 2 \quad 0]^\top$
3	$[2 \quad 2 \quad 2 \quad 2 \quad 2 \quad 2 \quad 2 \quad 1]^\top$
4	$[2 \quad 2 \quad 2 \quad 2 \quad 2 \quad 2 \quad 2 \quad 2]^\top$
$\vdots$	$\vdots$
390622	$[-2 \quad -2 \quad -2 \quad -2 \quad -2 \quad -2 \quad -2 \quad -2]^\top$
390623	$[-2 \quad -2 \quad -2 \quad -2 \quad -2 \quad -2 \quad -2 \quad -1]^\top$
390624	$[-2 \quad -2 \quad -2 \quad -2 \quad -2 \quad -2 \quad -2 \quad 1]^\top$
390625	$[-2 \quad -2 \quad -2 \quad -2 \quad -2 \quad -2 \quad -2 \quad 0]^\top$

can be categorized as a greedy method [60]. Therefore, our goal is to derive a low-complexity integer matrix

$$\mathbf{T} = \begin{bmatrix} \mathbf{t}_1 & \mathbf{t}_2 & \mathbf{t}_3 & \mathbf{t}_4 & \mathbf{t}_5 & \mathbf{t}_6 & \mathbf{t}_7 & \mathbf{t}_8 \end{bmatrix}^\top \tag{4}$$

such that its rows $\mathbf{t}_k^\top$, $k = 1, 2, \ldots, 8$, satisfy:

$$\mathbf{t}_k = \arg\min_{\mathbf{t} \in \mathscr{D}} \operatorname{error}(\mathbf{t}, \mathbf{c}_k), \quad k = 1, 2, \ldots, 8, \tag{5}$$

subject to constraints such as (i) low-complexity of the candidate vector $\mathbf{t}$ and (ii) orthogonality of the resulting matrix $\mathbf{T}$. The objective function $\operatorname{error}(\cdot,\cdot)$ returns a given error measure and $\mathscr{D}$ is a suitable search space.

3.2 Search Space

In order to obtain a low-complexity matrix $\mathbf{T}$, its entries must be computationally simple [3, 11]. We define the search space as the collection of 8-point vectors whose entries are in a set, say $\mathscr{P}$, of low-complexity elements. Therefore, we have the search space $\mathscr{D} = \mathscr{P}^8$. Some choices for $\mathscr{P}$ include: $\mathscr{P}_1 = \{0, \pm 1\}$ and $\mathscr{P}_2 = \{0, \pm 1, \pm 2\}$. Tables 3 and 4 display some elements of the search spaces $\mathscr{D}_1 = \mathscr{P}_1^8$ and $\mathscr{D}_2 = \mathscr{P}_2^8$. These search spaces have 6,561 and 390,625 elements, respectively.

3.3 Objective Function

The problem posed in (5) requires the identification of an error function to quantify the "distance" between the candidate row vectors from $\mathscr{D}$ and the rows of the exact DCT. Related literature often consider error functions based on matrix norms [46], proximity to orthogonality [61], and coding performance [3].

In this work, we propose the utilization of a distance based on the angle between vectors as the objective function to be minimized. Let $\mathbf{u}$ and $\mathbf{v}$ be two vectors defined over the same Euclidean space. The angle between vectors is simply given by:

$$\operatorname{angle}(\mathbf{u}, \mathbf{v}) = \arccos\left(\frac{\langle \mathbf{u}, \mathbf{v} \rangle}{\|\mathbf{u}\| \cdot \|\mathbf{v}\|} \right),$$

where $\langle \cdot, \cdot \rangle$ is the inner product and $\| \cdot \|$ indicates the norm induced by the inner product [62].

3.4 Orthogonality and Row Order

In addition, we require that the ensemble of rows $\mathbf{t}_k^\top$, $k = 1, 2, \ldots, 8$, must form an orthogonal set. This is to ensure that an orthogonal approximation can be obtained. As shown in [45, 47], for this property to be satisfied, it suffices that:

$$\mathbf{T} \cdot \mathbf{T}^\top = [\text{diagonal matrix}].$$

Because we aim at approximating each of the exact DCT matrix rows individually, the row sequential order according to which the approximations are performed may matter. Notice that we approximate the rows of the DCT based on a set of low-complexity rows, the search space. For instance, let us assume that we approximate the rows in the following order: $\wp = (1, 2, 3, 4, 5, 6, 7, 8)$. Once we find a good approximate row for the first exact row, i.e., a row vector in the search space which has the smallest angle in relation to that exact row, the second row is approximated considering only the row vectors in the search space that are orthogonal to the approximation for the first row. After that, the third exact row is approximated considering only the row vectors in the search space that are orthogonal to the first and second rows already chosen. And so on. This procedure characterize the greedy nature of the proposed algorithm.

Consider now the approximation order $(4, 3, 5, 6, 1, 2, 7, 8)$, a permutation of $\wp$. In this case, we start by approximating the fourth exact row considering the whole search space because we are starting from it. Hence, the obtained approximate row might be different from the one obtained by considering $\wp$, since in that case the search space is restricted in a different manner.

As an example, consider the DCT matrix of length 8, introduced in Section 2 of the manuscript. If considering the low complexity set $\{-1, 0, 1\}$ and the approximation order (1, 2, 3, 4, 5, 6, 7, 8) we obtain the following approximate matrix:

$$\begin{bmatrix} 1 & 1 & 1 & 1 & 1 & 1 & 1 & 1 \\ 1 & 1 & 1 & 0 & 0 & -1 & -1 & -1 \\ 1 & 0 & 0 & -1 & -1 & 0 & 0 & 1 \\ 1 & 0 & -1 & -1 & 1 & 1 & 0 & -1 \\ 1 & -1 & -1 & 1 & 1 & -1 & -1 & 1 \\ 1 & -1 & 0 & 1 & -1 & 0 & 1 & -1 \\ 0 & -1 & 1 & 0 & 0 & 1 & -1 & 0 \\ 0 & -1 & 1 & -1 & 1 & -1 & 1 & 0 \end{bmatrix}.$$

In other hand, if we consider the reverse approximation order, (8, 7, 6, 5, 4, 3, 2, 1), we obtain the following matrix:

$$\begin{bmatrix} 1 & 1 & 1 & 1 & 1 & 1 & 1 & 1 \\ 1 & 1 & 1 & 0 & 0 & -1 & -1 & -1 \\ 1 & 1 & -1 & -1 & -1 & -1 & 1 & 1 \\ 1 & 0 & -1 & -1 & 1 & 1 & 0 & -1 \\ 1 & -1 & -1 & 1 & 1 & -1 & -1 & 1 \\ 1 & -1 & 0 & 1 & -1 & 0 & 1 & -1 \\ 1 & -1 & 1 & -1 & -1 & 1 & -1 & 1 \\ 0 & -1 & 1 & -1 & 1 & -1 & 1 & 0 \end{bmatrix}.$$

Therefore, the row sequence considered matters for the resulting matrix. The sequence matters *during* the process of finding the approximate matrix.

Thus, the row vectors $\mathbf{c}_k^\top$ from the exact matrix must be approximated in all possibles sequences. For a systematic procedure, all the $8! = 40320$ possible permutations of the sequence $\wp$ must be considered.

```
procedure ABMAPPROX($\mathbf{C}$, $\wp$, $\mathscr{D}$)
    approximations $\leftarrow$ null 3D matrix of size $8 \times 8 \times n$;
    for $m \leftarrow 1, |\wp|$ do
        $\wp_m \leftarrow \wp(m,:)$
        for $k \leftarrow 1, 2, \ldots, 8$ do
            $\theta_{min} \leftarrow 2\pi$;
            $index \leftarrow 1$;
            for $i \leftarrow 1, 2, \ldots, |\mathscr{D}|$ do
                $aux \leftarrow$ approximations$(:,:,m) \cdot (\mathscr{D}(i,:))^\top$
                if $\operatorname{sum}(aux) = 0$ then
                    $\theta \leftarrow \operatorname{angle}(\mathbf{C}(\wp_m(k),:), \mathscr{D}(i,:))$;
                    if $\theta < \theta_{min}$ then
                        $\theta_{min} \leftarrow \theta$;
                        $index \leftarrow i$;
                    end if
                end if
            end for
            approximations$(\wp_m(k),: m) \leftarrow \mathscr{D}(index,:)$;
        end for
    end for
end procedure
```

Figure 1: Algorithm for the proposed method.

Let $\wp_m$, $m = 1, 2, \ldots, 40320$, be the resultant sequence that determines the mth permutation; e.g. $\wp_{1250} = (1, 3, 7, 6, 5, 4, 8, 2)$. The particular elements of a sequence are denoted by $\wp_m(k)$, $k = 1, 2, \ldots, 8$. Then, for the given example above, we have $\wp_{1250}(2) = 3$.

3.5 Proposed Optimization Problem

Considering the above discussion, we can re-cast (5) in more precise terms. For each permutation sequence $\wp_m$, we have the following optimization problem:

$$\mathbf{t}_{\wp_m(k)} = \arg\min_{\mathbf{d} \in \mathscr{D}} \operatorname{angle}(\mathbf{c}_{\wp_m(k)}, \mathbf{d}), \quad k = 1, 2, \ldots, 8, \tag{6}$$

subject to:

$$\langle \mathbf{t}_{\wp_m(i)}, \mathbf{t}_{\wp_m(j)} \rangle = 0, \quad i \neq j,$$

$m = 1, 2, \ldots, 40320$ and a fixed search space $\mathscr{D} \in \{\mathscr{D}_1, \mathscr{D}_2\}$. For each m, the solution of the above problem returns eight vectors, $\mathbf{t}^\top_{\wp_m(1)}, \mathbf{t}^\top_{\wp_m(2)}, \ldots, \mathbf{t}^\top_{\wp_m(8)}$, that are used as the rows of the desired low-complexity matrix. Note that each sequence $\wp_m$ may result in a different solution. Effectively, there are $8! = 40320$ problems to be solved. In principle, each permutation $\wp_m$ can furnish a different matrix.

Because the search space is relatively small, we solved (6) by means of exhaustive search. Although simple, such approach ensures the attainment of a solution and avoids convergence issues [60]. Figure 1 shows the pseudo-code for the adopted procedure to solve (6). It is important to highlight that although the proposed formulation is applicable to arbitrary transform lengths, it may not be computationally feasible. For this reason, we restrict our analysis to the 8-point case. Section 6.2 discusses an alternative form of generating higher order DCT approximations.

4 Results and Evaluation

In this section, we apply the proposed method aiming at the derivation of new approximations for the 8-point DCT. Subsequently, we analyze and compare the obtained matrices with a representative set of DCT approximations described in the literature according to several well-known figures of merit [63].

4.1 New 8-point DCT Approximations

Considering the search spaces $\mathscr{D}_1$ and $\mathscr{D}_2$ (cf. Table 3 and Table 4, respectively), we apply the proposed algorithm to solve (6). Because the first and fifth rows of the exact DCT are trivially approximated by the row vectors $\begin{bmatrix} 1 & 1 & 1 & 1 & 1 & 1 & 1 & 1 \end{bmatrix}$ and $\begin{bmatrix} 1 & -1 & -1 & 1 & 1 & -1 & -1 & 1 \end{bmatrix}$, respectively, we limited the search to the remaining six rows. As a consequence, the number of possible candidate matrices is reduced to $6! = 720$. For $\mathscr{D}_1$, only two different matrices were obtained, which coincide with previously archived approximations, namely: (i) the RDCT [27] and (ii) the matrix $\mathbf{T}_4$ introduced in [14]. These approximations are depicted in Table 2.

On the other hand, considering the search space $\mathscr{D}_2$, the following two new matrices were obtained:

$$\mathbf{T}_1 = \begin{bmatrix} 1 & 1 & 1 & 1 & 1 & 1 & 1 & 1 \\ 2 & 2 & 1 & 0 & 0 & -1 & -2 & -2 \\ 2 & 1 & -1 & -2 & -2 & -1 & 1 & 2 \\ 1 & 0 & -2 & -2 & 2 & 2 & 0 & -1 \\ 1 & -1 & -1 & 1 & 1 & -1 & -1 & 1 \\ 2 & -2 & 0 & 1 & -1 & 0 & 2 & -2 \\ 1 & -2 & 2 & -1 & -1 & 2 & -2 & 1 \\ 0 & -1 & 2 & -2 & 2 & -2 & 1 & 0 \end{bmatrix},$$

$$\mathbf{T}_2 = \begin{bmatrix} 1 & 1 & 1 & 1 & 1 & 1 & 1 & 1 \\ 2 & 1 & 2 & 0 & 0 & -2 & -1 & -2 \\ 2 & 1 & -1 & -2 & -2 & -1 & 1 & 2 \\ 2 & 0 & -2 & -1 & 1 & 2 & 0 & -2 \\ 1 & -1 & -1 & 1 & 1 & -1 & -1 & 1 \\ 1 & -2 & 0 & 2 & -2 & 0 & 2 & -1 \\ 1 & -2 & 2 & -1 & -1 & 2 & -2 & 1 \\ 0 & -2 & 1 & -2 & 2 & -1 & 2 & 0 \end{bmatrix}.$$

According to (1) and (2), the above *low-complexity* matrices $\mathbf{T}_1$ and $\mathbf{T}_2$ can be modified to provide orthogonal transformations $\widehat{\mathbf{C}}_1$ and $\widehat{\mathbf{C}}_2$. The selected orthogonalization procedure is based on the polar decomposition as described in [45, 47, 64]. Thus, the *orthogonal DCT approximations* associated to the matrices $\mathbf{T}_1$ and $\mathbf{T}_2$ are given by

$$\widehat{\mathbf{C}}_1 = \mathbf{S}_1 \cdot \mathbf{T}_1 \quad \text{and} \quad \widehat{\mathbf{C}}_2 = \mathbf{S}_2 \cdot \mathbf{T}_2,$$

where

$$\mathbf{S}_i = \sqrt{(\mathbf{T}_i \cdot \mathbf{T}_i{}^\top)^{-1}}, \quad i = 1, 2.$$

Thus, it follows that:

$$\mathbf{S}_1 = \mathbf{S}_2 = \operatorname{diag}\left(\frac{1}{\sqrt{8}}, \frac{1}{\sqrt{18}}, \frac{1}{\sqrt{20}}, \frac{1}{\sqrt{18}}, \frac{1}{\sqrt{8}}, \frac{1}{\sqrt{18}}, \frac{1}{\sqrt{20}}, \frac{1}{\sqrt{18}} \right).$$

Other simulations were performed considering extended sets of elements. In particular, following sets were considered: $\{0, \pm 1, \pm 4\}$, $\{0, \pm 1, \pm 8\}$, $\{0, \pm 1, \pm 2, \pm 4\}$, $\{0, \pm 1, \pm 2, \pm 8\}$, and $\{0, \pm 2, \pm 4, \pm 8\}$. Generally, the resulting matrices did not perform as well as the ones being proposed. Moreover, the associate computational cost was consistently higher.

The number of vectors in the search space can be calculated as $|\mathscr{D}| = |\mathscr{P}|^8$ (cf. Section 3.2). Therefore, including more elements to $\mathscr{P}$ effects a noticeable increase in the size of the search space. As a consequence, the processing time to derive all the 6! candidate matrices increases accordingly.

4.2 Approximation Measures

Approximations measurements are computed between an approximate matrix $\hat{\mathbf{C}}$ (not the low-complexity matrix $\mathbf{T}$) relative to the exact DCT. To evaluate the performance of the proposed approximations, $\widehat{\mathbf{C}}_1$ and $\widehat{\mathbf{C}}_2$, we selected traditional figures of merit: (i) total error energy ($\varepsilon(\cdot)$) [46]; (ii) mean square error (MSE$(\cdot)$) [3, 65]; (iii) coding gain ($C_g(\cdot)$) [3, 66, 67]; and (iv) transform efficiency ($\eta(\cdot)$) [3]. The MSE and total error energy are suitable measures to quantify the difference between the exact DCT and its approximations [3]. The coding gain and transform efficiency are appropriate tools to quantify compression, redundancy removal, and data decorrelation capabilities [3]. Additionally, due the angular nature of the objective function required by the proposed optimization problem, we also considered descriptive circular statistics [68, 69]. Circular statistics allows the quantification of approximation error in terms of the angle difference between the row vectors of the approximated and exact matrix.

Hereafter we adopt the following quantities and notation: the interpixel correlation is $\rho = 0.95$ [3, 35, 66], $\widehat{\mathbf{C}}$ is an approximation for the DCT, and $\widehat{\mathbf{R}}_\mathbf{y} = \widehat{\mathbf{C}} \cdot \mathbf{R}_\mathbf{x} \cdot \widehat{\mathbf{C}}^\top$, where $\mathbf{R}_\mathbf{x}$ is the covariance matrix of $\mathbf{x}$, whose elements are given by $\rho^{|i-j|}$, $i, j = 1, 2, \ldots, 8$. We detail each of these measures below.

4.2.1 Total Energy Error

The total energy error is a similarity measure given by [46]:

$$\varepsilon(\widehat{\mathbf{C}}) = \pi \cdot \|\mathbf{C} - \widehat{\mathbf{C}}\|_\mathrm{F}^2,$$

where $\|\cdot\|_\mathrm{F}$ represents the Frobenius norm [70].

4.2.2 Mean Square Error

The MSE of a given approximation $\widehat{\mathbf{C}}$ is furnished by [3, 65]:

$$\mathrm{MSE}(\widehat{\mathbf{C}}) = \frac{1}{8} \cdot \mathrm{tr}\left((\mathbf{C} - \widehat{\mathbf{C}}) \cdot \mathbf{R}_\mathbf{x} \cdot (\mathbf{C} - \widehat{\mathbf{C}})^\top \right).$$

where $\mathrm{tr}(\cdot)$ represents the trace operator [3]. The total energy error and the mean square error are appropriate measures for capturing the approximation error in a Euclidean distance sense.

4.2.3 Coding Gain

The coding gain quantifies the energy compaction capability and is given by [3]:

$$C_g(\widehat{\mathbf{C}}) = 10 \cdot \log_{10} \left\{ \frac{\frac{1}{8}\sum_{i=1}^{8} r_{i,i}}{\left(\prod_{i=1}^{8} r_{i,i} \cdot \|\widehat{\mathbf{c}}_i\|^2\right)^{1/8}} \right\},$$

where $r_{i,i}$ is the ith element of the diagonal of $\widehat{\mathbf{R}}_\mathbf{y}$ [3] and $\widehat{\mathbf{c}}_i^\top$ is the ith row of $\widehat{\mathbf{C}}$.

However, as pointed in [67], the previous definition is suitable for orthogonal transforms only. For non-orthogonal transforms, such as SDCT [51] and MRDCT [48], we adopt the unified coding gain [67]. For $i = 1, 2, \ldots, 8$, let $\widehat{\mathbf{c}}_i^\top$ and $\widehat{\mathbf{g}}_i^\top$ be ith row of $\widehat{\mathbf{C}}$ and $\widehat{\mathbf{C}}^{-1}$, respectively. Then, the unified coding gain is given by:

$$C_g^*(\widehat{\mathbf{C}}) = 10 \cdot \log_{10} \left\{ \prod_{i=1}^{8} \frac{1}{\sqrt[8]{A_i \cdot B_i}} \right\},$$

where $A_i = \mathrm{su}\left[\left(\widehat{\mathbf{c}}_i \cdot \widehat{\mathbf{c}}_i^\top \right) \odot \mathbf{R}_x \right]$, $\mathrm{su}(\cdot)$ returns the sum of all elements of the input matrix, the operator $\odot$ represents the element-wise product, and $B_i = \|\widehat{\mathbf{g}}_i\|^2$.

4.2.4 Transform Efficiency

The transform efficiency is an alternative measure to the coding gain, being expressed according to [3]:

$$\eta(\widehat{\mathbf{C}}) = \frac{\sum_{i=1}^{8} |r_{i,i}|}{\sum_{i=1}^{8} \sum_{j=1}^{8} |r_{i,j}|} \cdot 100,$$

where $r_{i,j}$ is the (i,j)th entry of $\widehat{\mathbf{R}}_\mathbf{y}$, $i, j = 1, 2, \ldots, 8$ [3].

4.2.5 Circular Statistics

Because the objective function in (6) is the operator angle, its associate values are distributed around the unit circle. This type of data is suitably analyzed by circular statistics tools [68, 69, 71]. Let $\mathbf{a}$ be an arbitrary 8-point vector and $\mathbf{q} = \begin{bmatrix} 1 & 0 & 0 & 0 & 0 & 0 & 0 & 0 \end{bmatrix}$. The angle function is given by [68]:

$$\theta = \mathrm{angle}(\mathbf{a}', \mathbf{q}), \quad k = 1, 2, \ldots, 8,$$

where $\mathbf{a}' = \frac{\mathbf{a}}{\|\mathbf{a}\|}$ is the normalized vector of $\mathbf{a}$.

The mean angle (circular mean) is given by [69, 71]:

$$\bar{\theta} = \begin{cases} \arctan(S/C), & \text{if } C > 0 \text{ and } S \geq 0, \\ \pi/2, & \text{if } C = 0 \text{ and } S > 0, \\ \arctan(S/C) + \pi, & \text{if } C < 0, \\ \arctan(S/C) + 2\pi, & \text{if } C \geq 0 \text{ and } S < 0, \\ \text{undefined}, & \text{if } C = 0 \text{ and } S = 0, \end{cases}$$

where $C = \sum_i \cos(\theta_i)$, $S = \sum_i \sin(\theta_i)$, and $\{\theta_i\}$ is a collection of angles. The circular variance is given by [68]:

$$V = 1 - \frac{\sqrt{C^2 + S^2}}{8}.$$

The minimal variance occurs when all observed angles are identical. In this case, we have $V = 0$. In other hand, the maximum variance occurs when the observations are uniformly distributed around the unit circle. Thus, $V = 1$ [69].

Considering the rows of the 8-point DCT matrix and of a given 8-point DCT approximate matrix, the angle function furnishes the following angles, respectively: $\theta_{\mathbf{c}_k} = \mathrm{angle}(\mathbf{c}_k, \mathbf{q})$ and $\theta_{\mathbf{t}_k} = \mathrm{angle}(\mathbf{t}_k, \mathbf{q})$, $k = 1, 2, \ldots, 8$ (cf. (3) and (4)). In this particular case, the mean circular difference, which measures the mean difference between the pairs of angles is defined as follows:

$$\bar{D} = \frac{1}{8^2} \cdot \sum_{i=1}^{8} \sum_{j=1}^{8} \left(\pi - |\pi - |\theta_{\mathbf{c}_i} - \theta_{\mathbf{t}_j}|| \right).$$

The expression above considers the difference between all the possible pairs of angles. However, we are interested in comparing the angle between the ith row of the DCT and the corresponding row of the approximated matrix, i.e., the cases where $i = j$. Thus we have the modified circular mean difference according to:

$$\bar{D}_{mod} = \frac{1}{8} \cdot \sum_{i=1}^{8} \left(\pi - |\pi - |\theta_{\mathbf{c}_i} - \theta_{\mathbf{t}_i}|| \right).$$

4.3 Results and Comparisons

Table 5 shows the obtained measurements for all approximations derived, according to (1), from the low-complexity matrices considered in this paper. Table 6 brings a summary of the descriptive circular statistics. We also included the exact DCT and the integer DCT (IDCT) [72] for comparison. The considered IDCT is the 8-point approximation

Table 5: Performance measures for DCT approximations derived from low-complexity matrices. Exact DCT measures listed for reference

Method	ε	MSE	C_g^*	η
DCT [12]	0	0	8.8259	93.9912
IDCT (HEVC) [72]	0.0020	8.66×10^{-6}	8.8248	93.8236
$\widehat{\mathbf{C}}_1$ (proposed)	1.2194	0.0046	8.6337	90.4615
$\widehat{\mathbf{C}}_2$ (proposed)	1.2194	0.0127	8.1024	87.2275
$\widehat{\mathbf{C}}_{\text{LO}}$ [57]	0.8695	0.0061	8.3902	88.7023
$\widehat{\mathbf{C}}_{\text{SDCT}}$ [51]	3.3158	0.0207	6.0261	82.6190
$\widehat{\mathbf{C}}_{\text{RDCT}}$ [27]	1.7945	0.0098	8.1827	87.4297
$\widehat{\mathbf{C}}_{\text{MRDCT}}$ [48]	8.6592	0.0594	7.3326	80.8969
$\widehat{\mathbf{C}}_{\text{BAS-2008a}}$ [53]	5.9294	0.0238	8.1194	86.8626
$\widehat{\mathbf{C}}_{\text{BAS-2008b}}$ [52]	4.1875	0.0191	6.2684	83.1734
$\widehat{\mathbf{C}}_{\text{BAS-2009}}$ [54]	6.8543	0.0275	7.9126	85.3799
$\widehat{\mathbf{C}}_{\text{BAS-2011}}$ [55]	26.8462	0.0710	7.9118	85.6419
$\widehat{\mathbf{C}}_{\text{BAS-2013}}$ [56]	35.0639	0.1023	7.9461	85.3138
$\widehat{\mathbf{C}}'_1$ [14]	3.3158	0.0208	6.0462	83.0814
$\widehat{\mathbf{C}}_4$ [14]	1.7945	0.0098	8.1834	87.1567
$\widehat{\mathbf{C}}_5$ [14]	1.7945	0.0100	8.1369	86.5359
$\widehat{\mathbf{C}}_6$ [14]	0.8695	0.0062	8.3437	88.0594

adopted in the HEVC standard [72]. A more detailed analysis on the performance of the proposed approximation in comparison with the IDCT is provided in Section 6.2. The proposed DCT approximation $\widehat{\mathbf{C}}_1$ outperforms all competing methods in terms of MSE, coding gain, and transform efficiency. It also performs as the second best for total error energy measurement. It is unusual for an approximation to simultaneously excel in measures based on Euclidean distance (ε and MSE) as well as in coding-based measures. The approximation by Lengwehasatit–Ortega ($\widehat{\mathbf{C}}_{\text{LO}}$) [57] achieves second best results MSE, and η. Because of its relatively inferior performance, we removed the new approximation $\widehat{\mathbf{C}}_2$ from our subsequent analysis. Nevertheless, $\widehat{\mathbf{C}}_2$ could outperform the approximations $\widehat{\mathbf{C}}_{\text{BAS-2008b}}$ [52], $\widehat{\mathbf{C}}_{\text{BAS-2009}}$ [54], $\widehat{\mathbf{C}}_{\text{BAS-2011}}$ [55], $\widehat{\mathbf{C}}_{\text{BAS-2013}}$ [56], $\widehat{\mathbf{C}}_{\text{SDCT}}$ [51], $\widehat{\mathbf{C}}_{\text{MRDCT}}$ [48], and $\widehat{\mathbf{C}}'_1$ [14] in all measures considered, $\widehat{\mathbf{C}}_4$ [14] and $\widehat{\mathbf{C}}_5$ [14] in terms of total error energy and transform efficiency, $\widehat{\mathbf{C}}_{\text{RDCT}}$ [27] in terms of total error energy, and $\widehat{\mathbf{C}}_{\text{BAS-2008a}}$ [53] in terms of total error energy, MSE and transform efficiency. Hereafter we focus our attention on the proposed approximation $\widehat{\mathbf{C}}_1$.

The proposed search algorithm is greedy, i.e., it makes local optimal choices hoping to find the global optimum solution [60]. Therefore, it is not guaranteed that the obtained solutions are globally optimal. This is exactly what happens here. As can be seen in Table 6, the proposed matrix $\mathbf{T}_1$ is not the transformation matrix that provides the lowest circular mean difference among the approximations on literature. Despite this fact, the proposed matrix has outstanding performance according to the considered measures.

Figure 2 shows the effect of the interpixel correlation ρ on the performance of the discussed approximate transforms as measured by the unified coding gain difference compared to the exact DCT [73]. The proposed method outperforms the competing methods as its coding gain difference is smaller for any choice of ρ. For highly correlated data the coding degradation in dB is roughly reduced by half when the proposed approximation $\widehat{\mathbf{C}}_1$ is considered.

5 Fast Algorithm and Hardware Realization

5.1 Fast Algorithm

The direct implementation of $\mathbf{T}_1$ requires 48 additions and 24 bit-shifting operations. However, such computational cost can be significantly reduced by means of sparse matrix factorization [11]. In fact, considering butterfly-based structures as commonly found in decimation-in-frequency algorithms, such as [5, 33, 74], we could derive the following factorization for $\mathbf{T}_1$:

Table 6: Descriptive circular statistics

Method	$\bar{\theta}$	V	$\bar{D}_{mod}$
Exact DCT [12]	70.53	0.0089	0
IDCT (HEVC) [72]	70.50	0.0086	0.0022
$\mathbf{T}_1$ (proposed)	71.12	0.0124	0.0711
$\mathbf{T}_2$ (proposed)	71.12	0.0124	0.0343
$\mathbf{T}_{\text{LO}}$ [57]	70.81	0.0102	0.0483
$\mathbf{T}_{\text{SDCT}}$ [51]	69.29	0	0.1062
$\mathbf{T}_{\text{RDCT}}$ [27]	71.98	0.0174	0.0716
$\mathbf{T}_{\text{MRDCT}}$ [48]	75.58	0.0392	0.1646
$\mathbf{T}_{\text{BAS-2008a}}$ [53]	72.35	0.0198	0.1036
$\mathbf{T}_{\text{BAS-2008b}}$ [52]	67.29	0.0015	0.1097
$\mathbf{T}_{\text{BAS-2009}}$ [54]	72.10	0.0183	0.1334
$\mathbf{T}_{\text{BAS-2011}}$ [55]	73.54	0.0265	0.1492
$\mathbf{T}_{\text{BAS-2013}}$ [56]	69.29	0	0.1062
$\mathbf{T}'_1$ [14]	73.54	0.0265	0.0901
$\mathbf{T}_4$ [14]	70.57	0.0085	0.0781
$\mathbf{T}_5$ [14]	72.45	0.0209	0.0730
$\mathbf{T}_6$ [14]	71.27	0.0139	0.0497

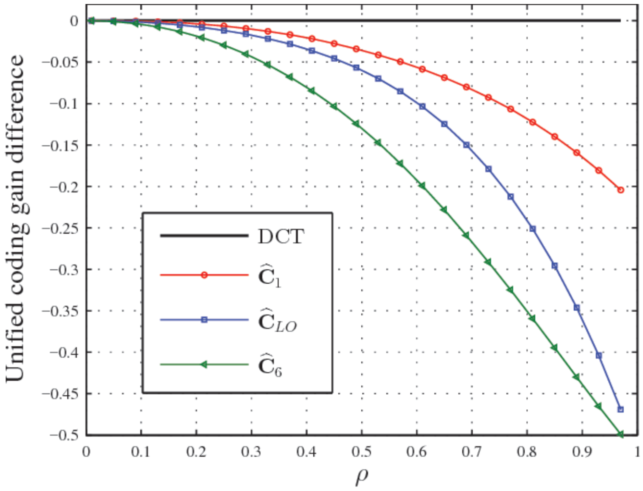

Figure 2: Curves for the coding gain error of $\widehat{\mathbf{C}}_1$, $\widehat{\mathbf{C}}_{\text{LO}}$, and $\widehat{\mathbf{C}}_6$, relative to the exact DCT, for $0 < \rho < 1$.

$$\mathbf{T}_1 = \mathbf{D} \cdot \mathbf{A}_4 \cdot \mathbf{A}_3 \cdot \mathbf{A}_2 \cdot \mathbf{A}_1,$$

where:

$$\mathbf{A}_1 = \begin{bmatrix} 1 & & & & & & & 1 \\ & 1 & & & & & 1 & \\ & & 1 & & & 1 & & \\ & & & 1 & 1 & & & \\ & & & 1 & -1 & & & \\ & & 1 & & & -1 & & \\ & 1 & & & & & -1 & \\ 1 & & & & & & & -1 \end{bmatrix}, \quad \mathbf{A}_2 = \begin{bmatrix} 1 & & & 1 & & & & \\ & 1 & 1 & & & & & \\ & 1 & -1 & & & & & \\ 1 & & & -1 & & & & \\ & & & & 1 & & & \\ & & & & & 1 & & \\ & & & & & & 1 & \\ & & & & & & & 1 \end{bmatrix},$$

$$\mathbf{A}_3 = \begin{bmatrix} 1 & 1 & & & & & & \\ 1 & -1 & & & & & & \\ & & 1 & & & & & \\ & & & 1 & & & & \\ & & & & 1 & & & \\ & & & & & 1 & & \\ & & & & & & 1 & \\ & & & & & & & 1 \end{bmatrix}, \quad \mathbf{A}_4 = \begin{bmatrix} 1 & & & & & & & \\ & & & & & \frac{1}{2} & 1 & 1 \\ & & 1 & 2 & & & & \\ & & & & -1 & -1 & & \frac{1}{2} \\ & 1 & & & & & & \\ & & & & \frac{1}{2} & & -1 & 1 \\ & & -2 & 1 & & & & \\ & & & & -1 & 1 & -\frac{1}{2} & \end{bmatrix},$$

and $\mathbf{D} = \text{diag}(1, 2, 1, 2, 1, 2, 1, 2)$. Figure 3 shows the signal flow graph (SFG) related to the above factorization. The computational cost of this algorithm is only 24 additions and six multiplications by two. The multiplications by two are extremely simple to be performed, requiring only bit-shifting operations [3]. The fast algorithm proposed requires 50% less additions and 75% less bit-shifting operations when

Table 7: Computational cost comparison

Method	Multiplications	Additions	Bit-shifts
DCT [23]	11	29	0
IDCT (HEVC) [72]	0	50	30
$\mathbf{T}_1$ (proposed)	0	24	6
$\mathbf{T}_{\text{LO}}$ [57]	0	24	2
$\mathbf{T}_{\text{SDCT}}$ [51]	0	24	0
$\mathbf{T}_{\text{RDCT}}$ [27]	0	22	0
$\mathbf{T}_{\text{MRDCT}}$ [48]	0	14	0
$\mathbf{T}_{\text{BAS-2008a}}$ [53]	0	18	2
$\mathbf{T}_{\text{BAS-2008b}}$ [52]	0	21	0
$\mathbf{T}_{\text{BAS-2009}}$ [54]	0	18	0
$\mathbf{T}_{\text{BAS-2011}}$ [55]	0	16	0
$\mathbf{T}_{\text{BAS-2013}}$ [56]	0	24	0
$\mathbf{T}_1^{'}$ [14]	0	18	0
$\mathbf{T}_4$ [14]	0	24	0
$\mathbf{T}_5$ [14]	0	24	4
$\mathbf{T}_6$ [14]	0	24	6

compared to the direct implementation. The computational costs of the considered methods are shown in Table 7. The additive cost of the discussed approximations varies from 14 to 28 additions.

In general terms, DCT approximations exhibit a trade-off between computational cost and transform performance [61], i.e., less complex matrices effect poor spectral approximations [3]. Departing from this general behavior, the proposed transformation $\mathbf{T_1}$ has (i) excelling performance measures and (ii) lower or similar arithmetic cost when compared to competing methods, as shown in Tables 5, 6, and 7. Regarding considered performance measures, three transformations are consistenly placed among the five best methods: $\mathbf{T}_1$, $\mathbf{T}_{\text{LO}}$, and $\mathbf{T}_6$. Thus, we separate them for hardware analysis.

5.2 FPGA Implementation

The proposed design along with $\mathbf{T}_{\text{LO}}$ and $\mathbf{T}_6$ were implemented on an FPGA chip using the Xilinx ML605 board. Considering hardware co-simulation the FPGA realization was tested with 100,000 random 8-point input test vectors. The test vectors were generated from within the MATLAB environment and, using JTAG based hardware co-simulation, routed to the physical FPGA device where each algorithm was realized in the reconfigurable logic fabric. Then the computational results obtained from the FPGA algorithm implementations were routed back to MATLAB memory space. The diagrams for the designs can be seen in Figure 4.

The metrics employed to evaluate the FPGA implementations were: configurable logic blocks (CLB), flip-flop (FF) count, and critical path delay (T_{cpd}), in ns. The maximum operating frequency was determined by the critical path delay as $F_{\max} = (T_{\text{cpd}})^{-1}$, in MHz. Values were obtained from the Xilinx FPGA synthesis and place-route tools by accessing the `xflow.results` report file. Using the Xilinx XPower Analyzer, we estimated the static (Q_p in W) and dynamic power (D_p in mW/MHz) consumption. In addition, we calculated area-time (AT) and area-time-square (AT^2) figures of merit, where area is measured as the CLBs and time as the critical path delay. The values of those metrics for each design are shown in Table 8.

The design linked to the proposed design approximation $\mathbf{T}_1$ possesses the smallest T_{cpd} among the considered methods. Such critical path delay allows for operations at a 8.55% and 19.96% higher frequency than the designs associated to $\mathbf{T}_{\text{LO}}$ and $\mathbf{T}_6$, respectively. In terms of area-time and are-time-square measures, the design linked to the approximation $\mathbf{T}_{\text{LO}}$ presents the best results, followed by the one associated to $\mathbf{T}_1$.

6 Computational Experiments

6.1 Still Image Compression

6.1.1 Experiment Setup and Results

To evaluate the efficiency of the proposed transformation matrix, we performed a JPEG-like image compression experiments as described in [14, 24, 27]. Input images were divided into sub-blocks of size 8×8 pixels and submitted to a bidimensional (2-D) transformation, such as the DCT or one of its approximations. Let $\mathbf{A}$ be a sub-block of size 8×8. The 2-D approximate transform of $\mathbf{A}$ is an 8×8 sub-block $\mathbf{B}$ obtained as follows [14, 46]:

$$\mathbf{B} = \widehat{\mathbf{C}} \cdot \mathbf{A} \cdot \widehat{\mathbf{C}}^{\top}.$$

Considering the zig-zag scan pattern as detailed in [75], the initial r elements of $\mathbf{B}$ were retained; whereas the remaining $(64 - r)$ elements were discarded. Considering 8-bit images, this approach implies that the fixed average bits per pixel equals $r/8$ bits per pixel (bpp). The previous operation results in a matrix $\mathbf{B}'$ populated with zeros which is suitable for entropy encoding [16]. Each processed sub-block was submitted to the corresponding 2-D inverse transformation and the image was reconstructed. For orthogonal approximations, the 2-D inverse transform is given by:

$$\mathbf{A} = \widehat{\mathbf{C}}^{\top} \cdot \mathbf{B}' \cdot \widehat{\mathbf{C}}.$$

We considered 44 standardized images obtained from the 'miscellaneous' volume from USC-SIPI image bank [76], which include common images such as *Lena*, *Boat*, *Baboon*, and *Peppers*. Without loss of generality, images were converted to 8-bit grayscale and submitted to the above described procedure. The reconstructed images were compared with the original images and evaluated quantitatively according to popular figures of merit: the mean square error (MSE) [3], the peak signal-to-noise ratio (PSNR) [63] and the structural similarity index (SSIM) [77]. We consider the MSE and PSNR measures because of its good properties and historical usage. However, as discussed in [65], the MSE and PSNR are not the best measures when it comes to predict human perception of image fidelity and quality, for which SSIM has been shown to be a better measure [65, 77].

Figure 5 shows the average MSE, PSNR, and SSIM respectively, for the 44 images considering $1 < r < 64$ (bpp from 0 to 8) retained coefficients. The proposed approximation $\widehat{\mathbf{C}}_1$ outperforms $\widehat{\mathbf{C}}_{\text{LO}}$ and $\widehat{\mathbf{C}}_6$ in terms of MSE and PSNR for any value of r. In terms of SSIM, $\widehat{\mathbf{C}}_1$ outperforms $\widehat{\mathbf{C}}_6$ for any value of r and $\widehat{\mathbf{C}}_{\text{LO}}$ for $r \in [7, 63]$.

In order to better visualize previous curves, we adopted the relative difference which is given by [78]:

$$RD = \frac{\mu(\mathbf{C}) - \mu(\widehat{\mathbf{C}})}{\mu(\mathbf{C})},$$

where $\mu(\mathbf{C})$ and $\mu(\widehat{\mathbf{C}})$ indicate measurements according to the exact and approximate DCT, respectively; and $\mu \in \{\text{MSE, PSNR, SSIM}\}$.

The relative difference for the MSE, PSNR, and SSIM are presented in Figure 6. Figure 6(c) shows that, for $12 < r < 60$ (bpp from 1.5 to 7.5), $\widehat{\mathbf{C}}_1$ outperforms not only $\widehat{\mathbf{C}}_{\text{LO}}$ and $\widehat{\mathbf{C}}_6$ but the DCT itself. To the best of our knowledge, this particularly good behavior was never described in literature, where invariably the performance of DCT approximations are routinely bounded by the performance of the exact DCT.

A qualitative evaluation is provided in Figures 7 and 8, where the reconstructed `Lena` images [76] for $r = 3$ (0.325 bpp) and $r = 14$ (1.75 bpp), respectively, according to the exact DCT, $\widehat{\mathbf{C}}_1$, $\widehat{\mathbf{C}}_{\text{LO}}$, and $\widehat{\mathbf{C}}_6$ are shown. As expected from the results shown in Figure 6(c), for a bitrate lower than 1.5, the proposed approximate transform matrix is not the

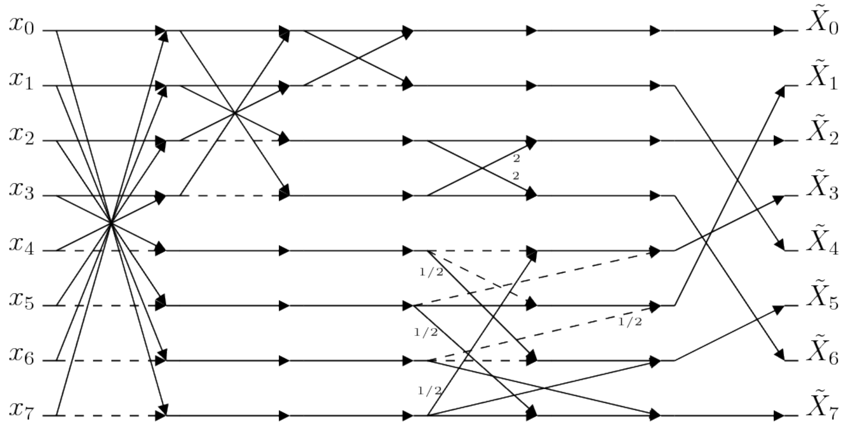

Figure 3: Signal flow graph of the proposed transform, relating the input data x_n, $n = 0,1,\ldots,7$, to its correspondent coefficients $\tilde{X}_k$, $k = 0,1,\ldots,7$, where $\tilde{\mathbf{X}} = \mathbf{x} \cdot \mathbf{T}_1$. of $\mathbf{T}_1$. Dashed arrows representing multiplication by -1.

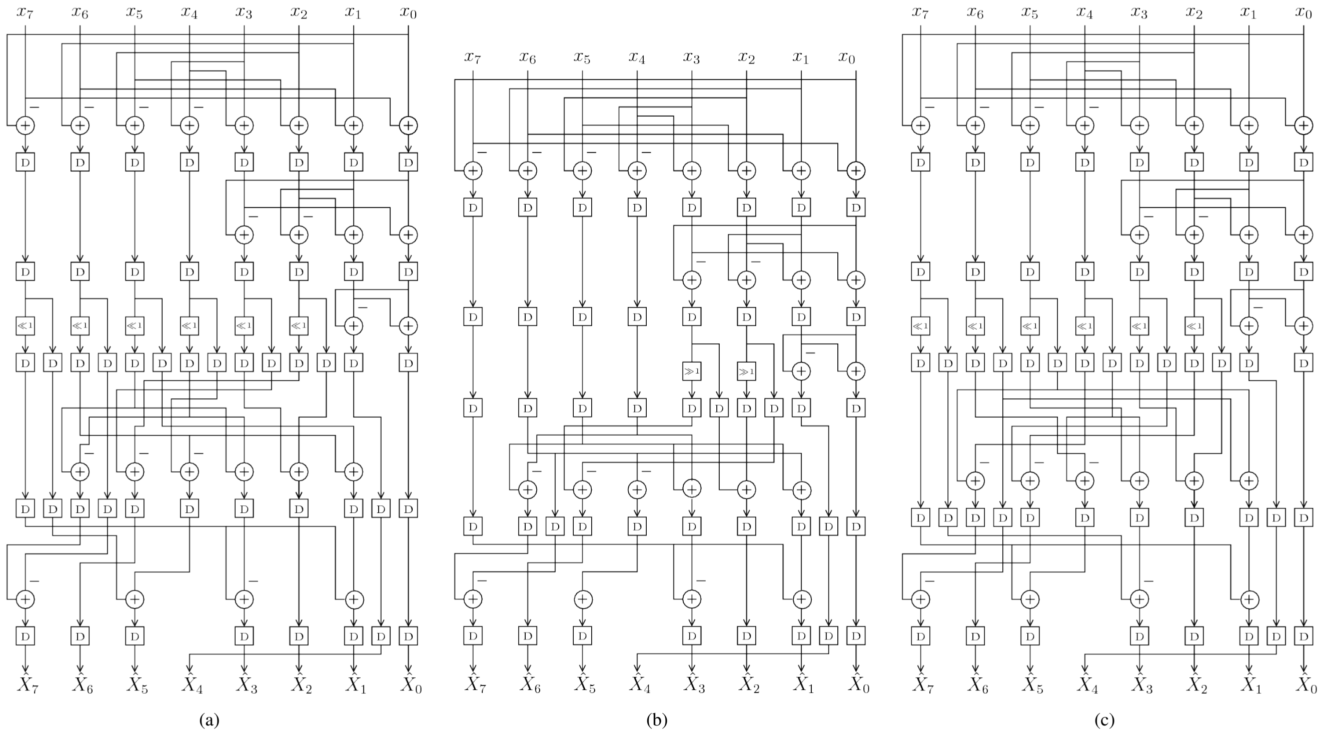

(a)

(b)

(c)

Figure 4: Architectures for (a) $\mathbf{T}_1$, (b) $\mathbf{T}_{\text{LO}}$, and (c) $\mathbf{T}_6$.

Table 8: Hardware resource consumption and power consumption using Xilinx Virtex-6 XC6VLX240T 1FFG1156 device

Approximation	CLB	FF	T_{cpd} (ns)	$F_{\max}$ (MHz)	D_p (mW/GHz)	Q_p (W)	AT	AT^2
$\mathbf{T}_1$ (proposed)	135	408	1.750	571	2.74	3.471	236	413
$\mathbf{T}_{\text{LO}}$ [57]	114	349	1.900	526	2.82	3.468	217	412
$\mathbf{T}_6$ [14]	125	389	2.100	476	2.57	3.460	262	551

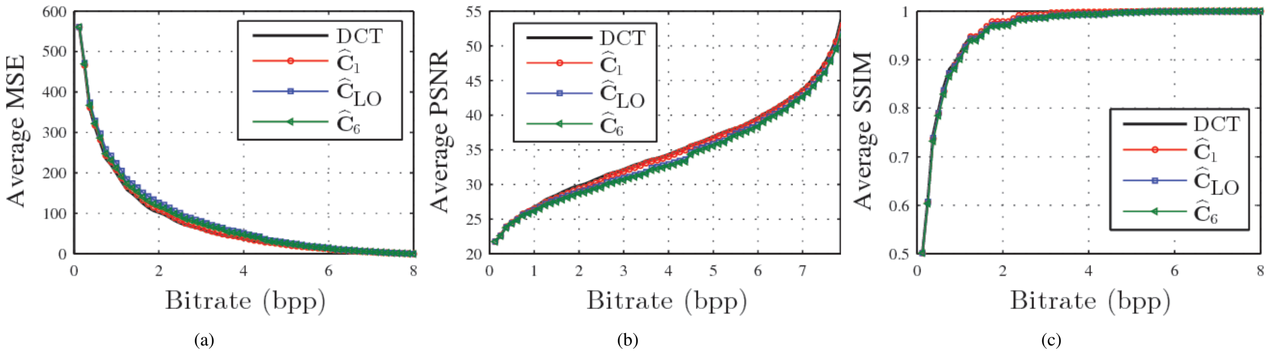

Figure 5: Curves for the average of (a) MSE; (b) PSNR; and (c) SSIM corresponding to 44 images.

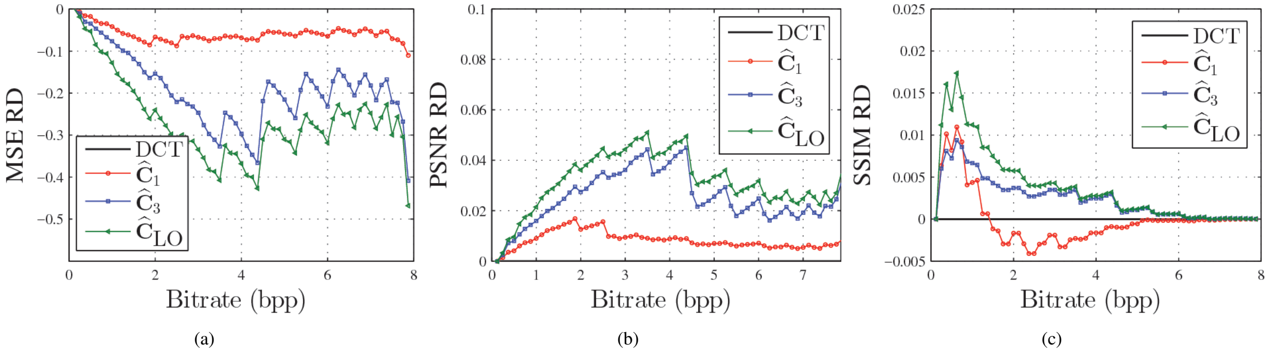

Figure 6: Relative difference curves for (a) MSE; (b) PSNR; and (c) SSIM of $\widehat{\mathbf{C}}_1$, $\widehat{\mathbf{C}}_{\mathrm{LO}}$, and $\widehat{\mathbf{C}}_6$, relative to the exact DCT.

one that performs the best (Figure 7), although the results are very similar to the ones furnished by the exact DCT. For a bitrate value larger than 1.5, Figure 8 demonstrates a situation were the proposed approximation overcomes the other transforms, including the DCT. In both cases, the visual difference between the DCT and the proposed aproximate transform matrix is very small.

6.1.2 Discussion

The obtained approximation was capable of outperforming the DCT under the above described conditions. We think that this is relevant, because it directly offers a counter-example to the belief that the coding performance of an approximation is supposed to always be inferior to the DCT. The theoretical background that leads the optimal performance of the DCT is based on assumption that the considered images must follow the Markov-1 processes with high correlation ($\rho \to 1$). In practice, natural images tend to fit under this assumption, but at lower correlation values the ideal case ($\rho \to 1$) may not necessarily be met as strongly. For instance, the average correlation of the considered image set was roughly 0.86. This practical deviation from the ideal case ($\rho \to 1$) may also play a role in explaining our results.

Finding matrix approximation as described in this work is a computational and numerical task. To the best of our knowledge, we cannot identify any methodology that could furnish necessary mathematical tools to design optimal approximations for image compression in an *a priori* manner, i.e., before search space approaches, optimization problem solving, or numerical simulation. In [3,5,25,61,79,80], a large number of methods is listed; all of them aim at good approximations. Although the problem of matrix approximation is quite simple to state, it is also very tricky and offers several non-linearities when combined to a more sophisticate system, such as image compression codecs. Finding low-complexity matrices can be categorized as an integer optimization problem. Thus, navigating in the low-complexity matrix search space might generate non-trivial performance curves, usually leading to discontinuities, which seems to be the case of the proposed approximations matrix $\mathbf{T}_1$. The navigation path through the search space is highly dependent on the search method and its objective function. Although approximation methods are very likely to provide reasonable approximations, it is also very hard to tell beforehand whether a given approximation method is capable of furnishing extremely good results capable of outperforming the state of the art. Only after experimentation with the obtained approximations one may know better. In particular, this work advances an optimization setup based on a geometrically intuitive objective function (angle between vectors) that could find good matrices as demonstrated by our *a posteriori* experiments.

6.2 Video Coding

In order to assess the proposed transform $\widehat{\mathbf{C}}_1$ as a tool for video coding, we embedded it into a public available HEVC reference software [81]. The HEVC presents several improvements relative to its predecessors [82] and aims at providing high compression rates [22]. Differently from other standards (cf. Section 1), HEVC employs not only an 8-point integer DCT (IDCT) but also transforms of size 4, 16, and 32 [72]. Such feature effects a series of optimization routines allowing the processing of big smooth or textureless areas [22].

The computational search used in the proposed method proved feasible for the 8-point case. However, as N increases, the size of the search space increases very quickly. For the case $N = 16$, if considering the low complexity set $\mathscr{P} = \{-1,0,1\}$, we have a search space with $3^{16} \approx 4.3 \times 10^7$ elements. For this blocklength, The proposed algorithm takes about 6 minutes to find an approximation for a fixed row

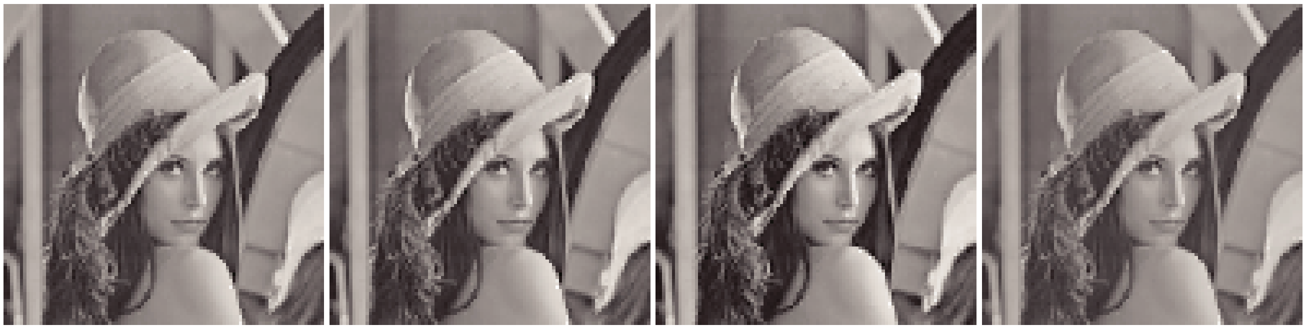

(a) MSE = 119.91, PSNR = 27.34, SSIM = 0.8814.

(b) MSE = 124.44, PSNR = 27.18, SSIM = 0.8767.

(c) MSE = 131.08, PSNR = 26.95, SSIM = 0.8781.

(d) MSE = 129.03, PSNR = 27.02, SSIM = 0.87.63.

Figure 7: Compression of `Lena` using (a) DCT; (b) $\widehat{\mathbf{C}}_1$; (c) $\widehat{\mathbf{C}}_{\mathrm{LO}}$; and (d) $\widehat{\mathbf{C}}_6$ considering $r = 3$ (0.325 bpp).

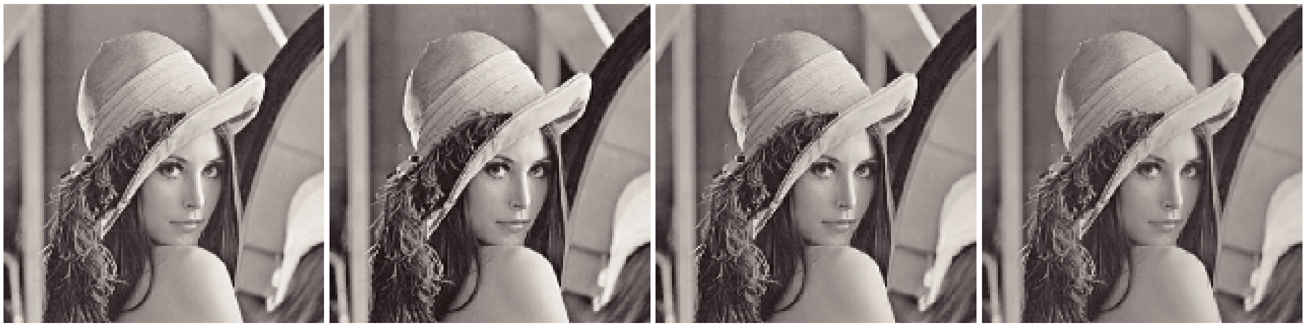

(a) MSE = 27.17, PSNR = 33.78, SSIM = 0.9888.

(b) MSE = 33.48, PSNR = 32.88, SSIM = 0.9893.

(c) MSE = 40.07, PSNR = 32.10, SSIM = 0.9849.

(d) MSE = 42.18, PSNR = 31.87, SSIM = 0.9844.

Figure 8: Compression of `Lena` using (a) DCT; (b) $\widehat{\mathbf{C}}_1$; (c) $\widehat{\mathbf{C}}_{\mathrm{LO}}$; and (d) $\widehat{\mathbf{C}}_6$ considering $r = 14$ (1.75).

sequence, considering a machine with the following specifications: 16-core 2.4 GHZ Intel(R) Xeon(R) CPU E5-2630 v3, with 32 GB RAM running Ubuntu 16.04.3 LTS 64-bit. Therefore, since we have $N!$ matrices to be generated, to run the whole algorithm would take approximately $16! \times 6$ minutes. In other words, the computation time would take an extremely large amount of time. Thus, for now, we limited the scope of our computational search to 8-point approximations.

For this reason, aiming to derive large blocklength transforms for HEVC embedding, we submitted the proposed transform matrix $\mathbf{T}_1$ to the Jridi–Alfalou–Meher (JAM) scalable algorithm [83]. Such method resulted in 16- and 32-point versions of the proposed matrix $\mathbf{T}_1$ that are suitable for the sought video experiments. Although the JAM algorithm is similar to Chen's DCT [30], it exploits redundancies allowing concise and high parallelizable hardware implementations [83]. From a low-complexity $N/2$-point transform, the JAM algorithm generates an $N \times N$ matrix transformation by combining two instantiations of the smaller one. The larger N-point transform is recursively defined by:

$$\mathbf{T}_{(N)} = \frac{1}{\sqrt{2}} \mathbf{M}_N^{\text{per}} \begin{bmatrix} \mathbf{T}_{(\frac{N}{2})} & \mathbf{Z}_{\frac{N}{2}} \\ \mathbf{Z}_{\frac{N}{2}} & \mathbf{T}_{(\frac{N}{2})} \end{bmatrix} \mathbf{M}_N^{\text{add}}, \tag{7}$$

where $\mathbf{Z}_{\frac{N}{2}}$ is a matrix of order $N/2$ with all zeroed entries. Matrices $\mathbf{M}_N^{\text{add}}$ and $\mathbf{M}_N^{\text{per}}$ are, respectively, obtained according to:

$$\mathbf{M}_N^{\text{add}} = \begin{bmatrix} \mathbf{I}_{\frac{N}{2}} & \bar{\mathbf{I}}_{\frac{N}{2}} \\ \bar{\mathbf{I}}_{\frac{N}{2}} & -\mathbf{I}_{\frac{N}{2}} \end{bmatrix}$$

and

$$\mathbf{M}_N^{\text{per}} = \begin{bmatrix} \mathbf{P}_{N-1,\frac{N}{2}} & \mathbf{Z}_{1,\frac{N}{2}} \\ \mathbf{Z}_{1,\frac{N}{2}} & \mathbf{P}_{N-1,\frac{N}{2}} \end{bmatrix},$$

where $\mathbf{I}_{\frac{N}{2}}$ and $\bar{\mathbf{I}}_{\frac{N}{2}}$ are, respectively, the identity and counter-identity matrices of order $N/2$ and $\mathbf{P}_{N-1,\frac{N}{2}}$ is an $(N-1) \times (N/2)$ matrix whose row vectors are defined by:

$$\mathbf{P}^{(i)}_{N-1,\frac{N}{2}} = \begin{cases} \mathbf{Z}_{1,\frac{N}{2}}, & \text{if } i = 1, 3, 5, \ldots, N-1 \\ \mathbf{I}^{(i/2)}_{\frac{N}{2}}, & \text{if } i = 0, 2, 4, \ldots, N-2. \end{cases}$$

The scaling factor $1/\sqrt{2}$ of (7) can be merged into the image/video compression quantization step. Furthermore, (1) can be applied to generate orthogonal versions of larger transforms. The computational cost of the resulting N-point transform is given by twice the number of bit-shifting operations of the original $N/2$-point transform; and twice the number of additions plus N extra additions. Following the described algorithm, we obtained the 16- and 32-point low complexity transform matrices proposed. More explicitly, we obtained the following 16- and 32-point matrices, respectively:

$$\mathbf{T}_{(16)} = \begin{bmatrix}
1 & 1 & 1 & 1 & 1 & 1 & 1 & 1 & 1 & 1 & 1 & 1 & 1 & 1 & 1 & 1 \\
1 & 1 & 1 & 1 & 1 & 1 & 1 & 1 & -1 & -1 & -1 & -1 & -1 & -1 & -1 & -1 \\
2 & 2 & 1 & 0 & 0 & -1 & -2 & -2 & -2 & -2 & -1 & 0 & 0 & 1 & 2 & 2 \\
2 & 2 & 1 & 0 & 0 & -1 & -2 & -2 & 2 & 2 & 1 & 0 & 0 & -1 & -2 & -2 \\
2 & 1 & -1 & -2 & -2 & -1 & 1 & 2 & 2 & 1 & -1 & -2 & -2 & -1 & 1 & 2 \\
2 & 1 & -1 & -2 & -2 & -1 & 1 & 2 & -2 & -1 & 1 & 2 & 2 & 1 & -1 & -2 \\
1 & 0 & -2 & -2 & 2 & 2 & 0 & -1 & -1 & 0 & 2 & 2 & -2 & -2 & 0 & 1 \\
1 & 0 & -2 & -2 & 2 & 2 & 0 & -1 & 1 & 0 & -2 & -2 & 2 & 2 & 0 & -1 \\
1 & -1 & -1 & 1 & 1 & -1 & -1 & 1 & 1 & -1 & -1 & 1 & 1 & -1 & -1 & 1 \\
1 & -1 & -1 & 1 & 1 & -1 & -1 & 1 & -1 & 1 & 1 & -1 & -1 & 1 & 1 & -1 \\
2 & -2 & 0 & 1 & -1 & 0 & 2 & -2 & -2 & 2 & 0 & -1 & 1 & 0 & -2 & 2 \\
2 & -2 & 0 & 1 & -1 & 0 & 2 & -2 & 2 & -2 & 0 & 1 & -1 & 0 & 2 & -2 \\
1 & -2 & 2 & -1 & -1 & 2 & -2 & 1 & 1 & -2 & 2 & -1 & -1 & 2 & -2 & 1 \\
1 & -2 & 2 & -1 & -1 & 2 & -2 & 1 & -1 & 2 & -2 & 1 & 1 & -2 & 2 & -1 \\
0 & -1 & 2 & -2 & 2 & -2 & 1 & 0 & 0 & 1 & -2 & 2 & -2 & 2 & -1 & 0 \\
0 & -1 & 2 & -2 & 2 & -2 & 1 & 0 & 0 & -1 & 2 & -2 & 2 & -2 & 1 & 0
\end{bmatrix}$$

and

$$\mathbf{T}_{(32)} =$$

$$\begin{bmatrix}
1 & 1 & 1 & 1 & 1 & 1 & 1 & 1 & 1 & 1 & 1 & 1 & 1 & 1 & 1 & 1 & 1 & 1 & 1 & 1 & 1 & 1 & 1 & 1 & 1 & 1 & 1 & 1 & 1 & 1 & 1 & 1 \\
1 & 1 & 1 & 1 & 1 & 1 & 1 & 1 & 1 & 1 & 1 & 1 & 1 & 1 & 1 & 1 & -1 & -1 & -1 & -1 & -1 & -1 & -1 & -1 & -1 & -1 & -1 & -1 & -1 & -1 & -1 & -1 \\
1 & 1 & 1 & 1 & 1 & 1 & 1 & 1 & -1 & -1 & -1 & -1 & -1 & -1 & -1 & -1 & -1 & -1 & -1 & -1 & -1 & -1 & -1 & -1 & 1 & 1 & 1 & 1 & 1 & 1 & 1 & 1 \\
1 & 1 & 1 & 1 & 1 & 1 & 1 & 1 & -1 & -1 & -1 & -1 & -1 & -1 & -1 & -1 & 1 & 1 & 1 & 1 & 1 & 1 & 1 & 1 & -1 & -1 & -1 & -1 & -1 & -1 & -1 & -1 \\
2 & 2 & 1 & 0 & 0 & -1 & -2 & -2 & -2 & -2 & -1 & 0 & 0 & 1 & 2 & 2 & 2 & 2 & 1 & 0 & 0 & -1 & -2 & -2 & -2 & -2 & -1 & 0 & 0 & 1 & 2 & 2 \\
2 & 2 & 1 & 0 & 0 & -1 & -2 & -2 & -2 & -2 & -1 & 0 & 0 & 1 & 2 & 2 & -2 & -2 & -1 & 0 & 0 & 1 & 2 & 2 & 2 & 2 & 1 & 0 & 0 & -1 & -2 & -2 \\
2 & 2 & 1 & 0 & 0 & -1 & -2 & -2 & 2 & 2 & 1 & 0 & 0 & -1 & -2 & -2 & -2 & -2 & -1 & 0 & 0 & 1 & 2 & 2 & -2 & -2 & -1 & 0 & 0 & 1 & 2 & 2 \\
2 & 2 & 1 & 0 & 0 & -1 & -2 & -2 & 2 & 2 & 1 & 0 & 0 & -1 & -2 & -2 & 2 & 2 & 1 & 0 & 0 & -1 & -2 & -2 & 2 & 2 & 1 & 0 & 0 & -1 & -2 & -2 \\
2 & 1 & -1 & -2 & -2 & -1 & 1 & 2 & 2 & 1 & -1 & -2 & -2 & -1 & 1 & 2 & 2 & 1 & -1 & -2 & -2 & -1 & 1 & 2 & 2 & 1 & -1 & -2 & -2 & -1 & 1 & 2 \\
2 & 1 & -1 & -2 & -2 & -1 & 1 & 2 & 2 & 1 & -1 & -2 & -2 & -1 & 1 & 2 & -2 & -1 & 1 & 2 & 2 & 1 & -1 & -2 & -2 & -1 & 1 & 2 & 2 & 1 & -1 & -2 \\
2 & 1 & -1 & -2 & -2 & -1 & 1 & 2 & -2 & -1 & 1 & 2 & 2 & 1 & -1 & -2 & -2 & -1 & 1 & 2 & 2 & 1 & -1 & -2 & 2 & 1 & -1 & -2 & -2 & -1 & 1 & 2 \\
2 & 1 & -1 & -2 & -2 & -1 & 1 & 2 & -2 & -1 & 1 & 2 & 2 & 1 & -1 & -2 & 2 & 1 & -1 & -2 & -2 & -1 & 1 & 2 & -2 & -1 & 1 & 2 & 2 & 1 & -1 & -2 \\
1 & 0 & -2 & -2 & 2 & 2 & 0 & -1 & -1 & 0 & 2 & 2 & -2 & -2 & 0 & 1 & 1 & 0 & -2 & -2 & 2 & 2 & 0 & -1 & -1 & 0 & 2 & 2 & -2 & -2 & 0 & 1 \\
1 & 0 & -2 & -2 & 2 & 2 & 0 & -1 & -1 & 0 & 2 & 2 & -2 & -2 & 0 & 1 & -1 & 0 & 2 & 2 & -2 & -2 & 0 & 1 & 1 & 0 & -2 & -2 & 2 & 2 & 0 & -1 \\
1 & 0 & -2 & -2 & 2 & 2 & 0 & -1 & 1 & 0 & -2 & -2 & 2 & 2 & 0 & -1 & -1 & 0 & 2 & 2 & -2 & -2 & 0 & 1 & -1 & 0 & 2 & 2 & -2 & -2 & 0 & 1 \\
1 & 0 & -2 & -2 & 2 & 2 & 0 & -1 & 1 & 0 & -2 & -2 & 2 & 2 & 0 & -1 & 1 & 0 & -2 & -2 & 2 & 2 & 0 & -1 & 1 & 0 & -2 & -2 & 2 & 2 & 0 & -1 \\
1 & -1 & -1 & 1 & 1 & -1 & -1 & 1 & 1 & -1 & -1 & 1 & 1 & -1 & -1 & 1 & 1 & -1 & -1 & 1 & 1 & -1 & -1 & 1 & 1 & -1 & -1 & 1 & 1 & -1 & -1 & 1 \\
1 & -1 & -1 & 1 & 1 & -1 & -1 & 1 & 1 & -1 & -1 & 1 & 1 & -1 & -1 & 1 & -1 & 1 & 1 & -1 & -1 & 1 & 1 & -1 & -1 & 1 & 1 & -1 & -1 & 1 & 1 & -1 \\
1 & -1 & -1 & 1 & 1 & -1 & -1 & 1 & -1 & 1 & 1 & -1 & -1 & 1 & 1 & -1 & -1 & 1 & 1 & -1 & -1 & 1 & 1 & -1 & 1 & -1 & -1 & 1 & 1 & -1 & -1 & 1 \\
1 & -1 & -1 & 1 & 1 & -1 & -1 & 1 & -1 & 1 & 1 & -1 & -1 & 1 & 1 & -1 & 1 & -1 & -1 & 1 & 1 & -1 & -1 & 1 & -1 & 1 & 1 & -1 & -1 & 1 & 1 & -1 \\
2 & -2 & 0 & 1 & -1 & 0 & 2 & -2 & -2 & 2 & 0 & -1 & 1 & 0 & -2 & 2 & 2 & -2 & 0 & 1 & -1 & 0 & 2 & -2 & -2 & 2 & 0 & -1 & 1 & 0 & -2 & 2 \\
2 & -2 & 0 & 1 & -1 & 0 & 2 & -2 & -2 & 2 & 0 & -1 & 1 & 0 & -2 & 2 & -2 & 2 & 0 & -1 & 1 & 0 & -2 & 2 & 2 & -2 & 0 & 1 & -1 & 0 & 2 & -2 \\
2 & -2 & 0 & 1 & -1 & 0 & 2 & -2 & 2 & -2 & 0 & 1 & -1 & 0 & 2 & -2 & -2 & 2 & 0 & -1 & 1 & 0 & -2 & 2 & -2 & 2 & 0 & -1 & 1 & 0 & -2 & 2 \\
2 & -2 & 0 & 1 & -1 & 0 & 2 & -2 & 2 & -2 & 0 & 1 & -1 & 0 & 2 & -2 & 2 & -2 & 0 & 1 & -1 & 0 & 2 & -2 & 2 & -2 & 0 & 1 & -1 & 0 & 2 & -2 \\
1 & -2 & 2 & -1 & -1 & 2 & -2 & 1 & 1 & -2 & 2 & -1 & -1 & 2 & -2 & 1 & 1 & -2 & 2 & -1 & -1 & 2 & -2 & 1 & 1 & -2 & 2 & -1 & -1 & 2 & -2 & 1 \\
1 & -2 & 2 & -1 & -1 & 2 & -2 & 1 & 1 & -2 & 2 & -1 & -1 & 2 & -2 & 1 & -1 & 2 & -2 & 1 & 1 & -2 & 2 & -1 & -1 & 2 & -2 & 1 & 1 & -2 & 2 & -1 \\
1 & -2 & 2 & -1 & -1 & 2 & -2 & 1 & -1 & 2 & -2 & 1 & 1 & -2 & 2 & -1 & -1 & 2 & -2 & 1 & 1 & -2 & 2 & -1 & 1 & -2 & 2 & -1 & -1 & 2 & -2 & 1 \\
1 & -2 & 2 & -1 & -1 & 2 & -2 & 1 & -1 & 2 & -2 & 1 & 1 & -2 & 2 & -1 & 1 & -2 & 2 & -1 & -1 & 2 & -2 & 1 & -1 & 2 & -2 & 1 & 1 & -2 & 2 & -1 \\
0 & -1 & 2 & -2 & 2 & -2 & 1 & 0 & 0 & 1 & -2 & 2 & -2 & 2 & -1 & 0 & 0 & -1 & 2 & -2 & 2 & -2 & 1 & 0 & 0 & 1 & -2 & 2 & -2 & 2 & -1 & 0 \\
0 & -1 & 2 & -2 & 2 & -2 & 1 & 0 & 0 & 1 & -2 & 2 & -2 & 2 & -1 & 0 & 0 & 1 & -2 & 2 & -2 & 2 & -1 & 0 & 0 & -1 & 2 & -2 & 2 & -2 & 1 & 0 \\
0 & -1 & 2 & -2 & 2 & -2 & 1 & 0 & 0 & -1 & 2 & -2 & 2 & -2 & 1 & 0 & 0 & 1 & -2 & 2 & -2 & 2 & -1 & 0 & 0 & 1 & -2 & 2 & -2 & 2 & -1 & 0 \\
0 & -1 & 2 & -2 & 2 & -2 & 1 & 0 & 0 & -1 & 2 & -2 & 2 & -2 & 1 & 0 & 0 & -1 & 2 & -2 & 2 & -2 & 1 & 0 & 0 & -1 & 2 & -2 & 2 & -2 & 1 & 0
\end{bmatrix}.$$

The resulting approximations for the above low-complexity matrices can be found from (1) and (2). The diagonal matrices implied by (2) are $\mathbf{D}_{(16)} = 4 \cdot \left[\begin{smallmatrix} 1 & 0 \\ 0 & 1 \end{smallmatrix}\right] \otimes \operatorname{diag}(4, 9, 10, 9) \otimes \left[\begin{smallmatrix} 1 & 0 \\ 0 & 1 \end{smallmatrix}\right]$ and $\mathbf{D}_{(32)} = 2 \cdot \mathbf{D}_{(16)} \otimes \left[\begin{smallmatrix} 1 & 0 \\ 0 & 1 \end{smallmatrix}\right]$, respectively, where $\otimes$ is the Kronecker product [50].

Figures 9 and 10 display the SFG for the low-complexity transform matrices $\mathbf{T}_{(16)}$ and $\mathbf{T}_{(32)}$ derived from $\mathbf{T}_1$.

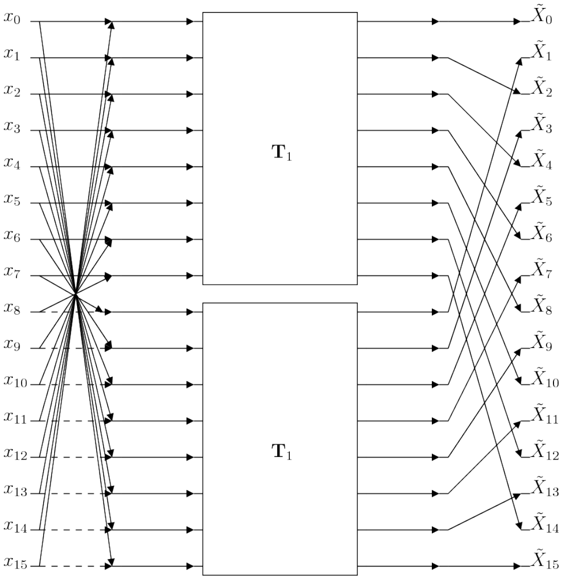

Figure 9: SFG for the proposed 16-point low complexity transform matrix.

Table 9 lists the computational costs of the proposed transform for sizes $N = 8, 16, 32$ compared to an efficient implementation of the IDCT [84].

In our experiments, the original 8-, 16-, and 32-point integer transforms of HEVC were substituted by $\widehat{\mathbf{C}}_1$ and its scaled versions. The original 4-point transform was kept unchanged because it is already a very low-complexity transformation. We encoded the first 100 frames of one video sequence of each A to F class in accordance with the common test conditions (CTC) documentation [85]. Namely we used the 8-bit videos: `PeopleOnStreet` (2560×1600 at 30 fps), `BasketballDrive` (1920×1080 at 50 fps), `RaceHorses` (832×480 at 30 fps), `BlowingBubbles` (416×240 at 50 fps), `KristenAndSara` (1280×720 at 60 fps), and `BasketbalDrillText` (832×480 at 50 fps).

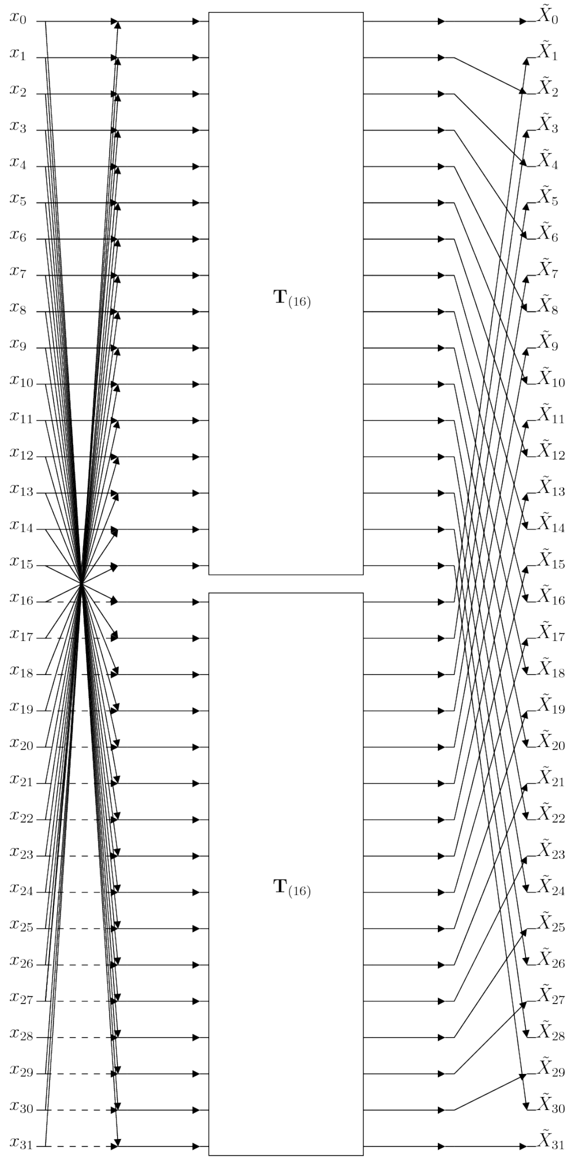

Figure 10: SFG for the proposed 32-point low complexity transform matrix, where $\mathbf{T}_{(16)}$ is the 16-point matrix presented in Figure 9.

As suggested in [83], all the test parameters were set according to the CTC documentation. We tested the proposed transforms in All Intra (AI), `Random Access` (RA), `Low Delay B` (LD-B), and `Low Delay P` (LD-P) configurations, all in the `Main` profile.

We selected the frame-by-frame MSE and PSNR [72] for each YUV color channel as figures of merit. Then, for all test videos, we computed the rate distortion (RD) curve considering the recommended quantization parameter (QP) values, i.e. 22, 27, 32, and 37 [85]. The resulting RD curves are depicted in Figure 11. We have also measured the Bjøntegaard's delta PSNR (BD-PSNR) and delta rate (BD-Rate) [86,87] for the modified HEVC software. These values are summarized in Table 10. We demonstrate that replacing the IDCT by the proposed transform and its scaled versions results in a loss in quality of at most 0.47dB for the AI configuration, which corresponds to an increase of 5.82% in bitrate. Worst performance for the other configurations—RA, LD-B, and LD-P—are found for the `KristenAndSara` video sequence, where approximately 0.55dB are lost if compared to the original HEVC implementation.

Table 9: Computational cost comparison for 8-, 16-, and 32-point transforms embedded in HEVC reference software

N	IDCT [84]		Proposed transform	
	Additions	Bit-shifts	Additions	Bit-shifts
8	50	30	24	6
16	186	86	64	12
32	682	278	160	24

Despite the very low computational cost when compared to the IDCT (cf. Table 9), the proposed transform does not introduce significant errors. Figure 12 illustrates the tenth frame of the `BasketballDrive` video encoded according to the default HEVC IDCT and $\widehat{\mathbf{C}}_1$ and its scaled versions for each coding configuration. The QP was set to 32. Visual degradations are virtually nonperceptible demonstrating real-world applicability of the proposed DCT approximations for high resolution video coding.

7 Conclusion

In this paper, we set up and solved an optimization problem aiming at the proposition of new approximations for the 8-point DCT. The obtained approximations were determined according to a greedy heuristic which minimized the angle between the rows of the approximate and the exact DCT matrices. Constraints of orthogonality and low computational complexity were imposed. One of the obtained approximations outperformed all the considered approximations in literature according to popular performance measures. We also introduced the use of circular statistics for assessing approximate transforms. For the proposed transform $\mathbf{T}_1$, a fast algorithm requiring only 24 additions and 6 bit-shifting operations was proposed. The fast algorithm for the proposed method and directly competing approximations were given FPGA realizations. Simulations were made and the hardware resource consumption and power consumption were measured. The maximum operating frequency of the proposed method was 37.4% higher when compared with the well-known Lengwehasatit–Ortega approximation (LO) [57]. In addition, the applicability of the proposed approximation in the context of image compression and video coding was demonstrated. Our experiments also demonstrate that DCT approximations can effectively approximate the DCT behavior, but also—under particular conditions—outperform the DCT itself for image coding. The proposed approximation is fully HEVC-compliant, being capable of video coding with HEVC quality at lower computational costs.

References

[1] G. H. Dunteman, *Principal components analysis*. Sage, 1989, vol. 69. 1

[2] I. Jolliffe, *Principal component analysis*. Wiley Online Library, 2002. 1

[3] V. Britanak, P. Yip, and K. R. Rao, *Discrete Cosine and Sine Transforms*. Academic Press, 2007. 1, 2, 3, 5, 6, 7, 9

[4] A. N. Gorban, B. Kgl, D. C. Wunsch, and A. Zinovyev, *Principal Manifolds for Data Visualization and Dimension Reduction*, 1st ed. Springer Publishing Company, Incorporated, 2007. 1

[5] K. R. Rao and P. Yip, *Discrete Cosine Transform: Algorithms, Advantages, Applications*. San Diego, CA: Academic Press, 1990. 1, 6, 9

[6] H. Chen and B. Zeng, "New transforms tightly bounded by DCT and KLT," *IEEE Signal Processing Letters*, vol. 19, no. 6, pp. 344–347, 2012. 1

[7] S. Álvarez-Cortés, N. Amrani, M. Hernández-Cabronero, and J. Serra-Sagristà, "Progressive lossy-to-lossless coding of hyperspectral images through regression wavelet analysis," *International Journal of Remote Sensing*, pp. 1–21, 2017. 1

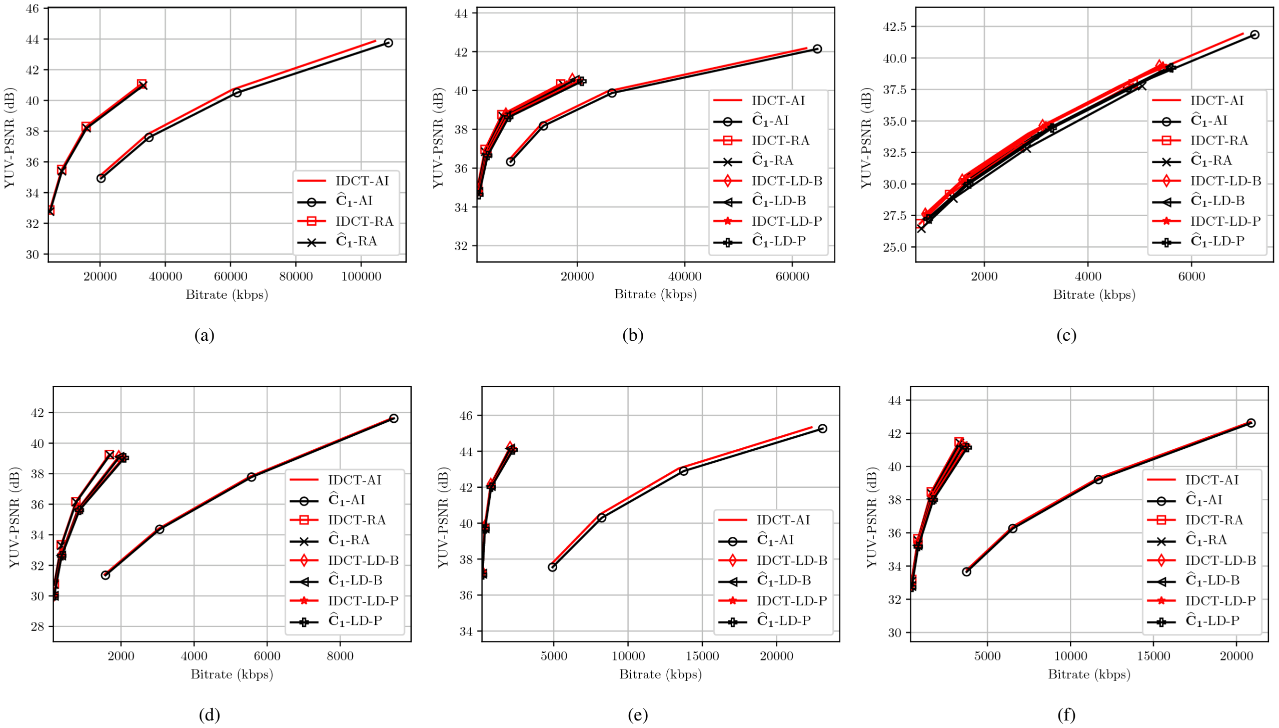

(a)

(b)

(c)

(d)

(e)

(f)

Figure 11: Rate distortion curves of the modified HEVC software for test sequences: (a) `PeopleOnStreet`, (b) `BasketballDrive`, (c) `RaceHorses`, (d) `BlowingBubbles`, (e) `KristenAndSara`, and (f) `BasketbalDrillText`.

Table 10: BD-PSNR (dB) and BD-Rate (%) of the modified HEVC reference software for tested video sequences

Video sequence	AI		RA		LD-B		LD-P	
	BD-PSNR	BD-Rate	BD-PSNR	BD-Rate	BD-PSNR	BD-Rate	BD-PSNR	BD-Rate
`PeopleOnStreet`	0.2999	−5.5375	0.1467	−3.4323	N/A	N/A	N/A	N/A
`BasketballDrive`	0.1692	−6.1033	0.1412	−6.1876	0.1272	−5.2730	0.1276	−5.2407
`RaceHorses`	0.4714	−5.8250	0.5521	−8.6149	0.5460	−7.9067	0.5344	−7.6868−
`BlowingBubbles`	0.0839	−1.4715	0.0821	−2.1612	0.0806	−2.1619	0.0813	−2.2370
`KristenAndSara`	0.2582	−5.0441	N/A	N/A	0.1230	−4.1823	0.1118	−4.0048
`BasketballDrillText`	0.1036	−1.9721	0.1372	−3.2741	0.1748	−4.3383	0.1646	−4.1509

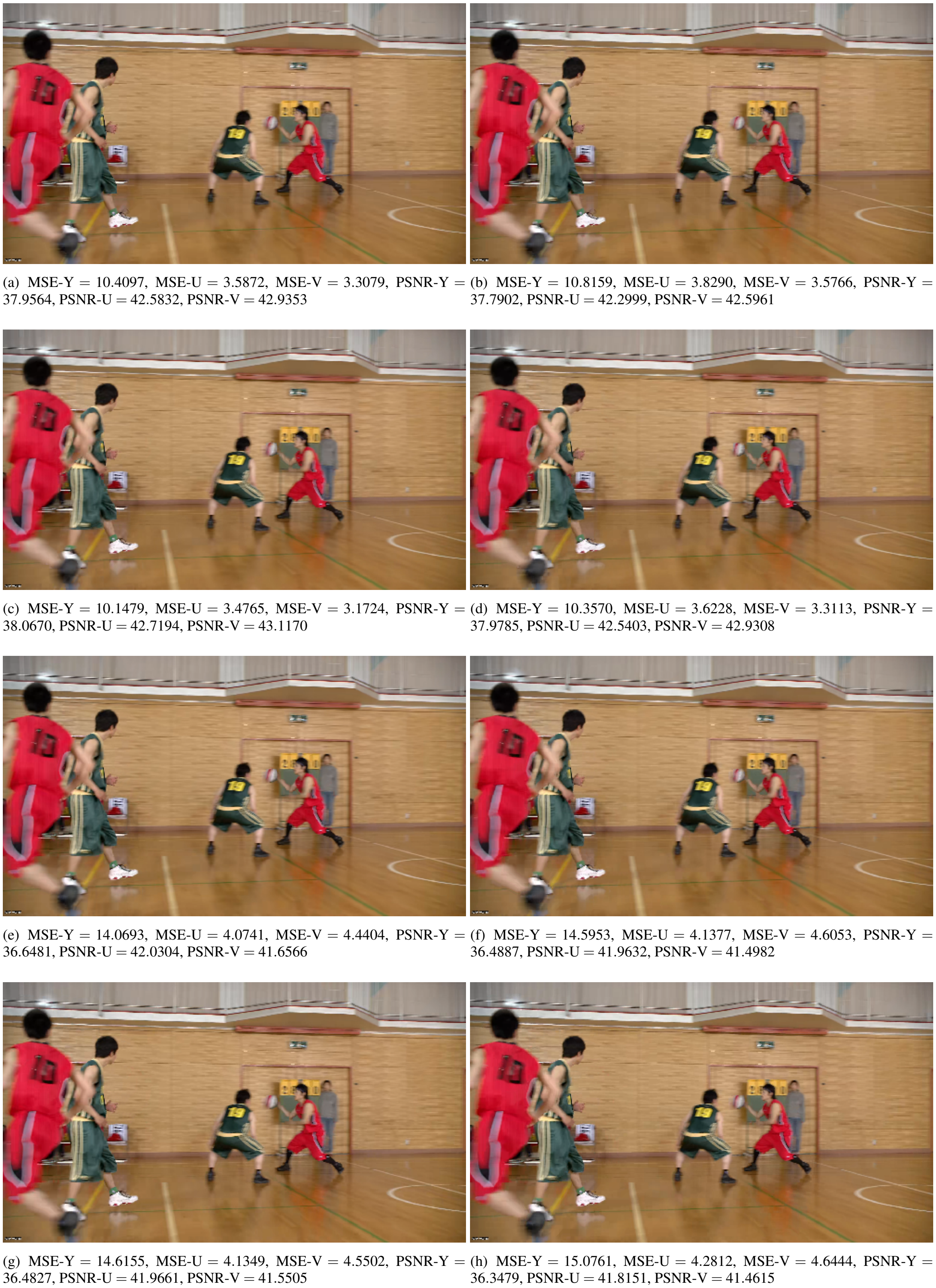

(a) MSE-Y = 10.4097, MSE-U = 3.5872, MSE-V = 3.3079, PSNR-Y = 37.9564, PSNR-U = 42.5832, PSNR-V = 42.9353

(b) MSE-Y = 10.8159, MSE-U = 3.8290, MSE-V = 3.5766, PSNR-Y = 37.7902, PSNR-U = 42.2999, PSNR-V = 42.5961

(c) MSE-Y = 10.1479, MSE-U = 3.4765, MSE-V = 3.1724, PSNR-Y = 38.0670, PSNR-U = 42.7194, PSNR-V = 43.1170

(d) MSE-Y = 10.3570, MSE-U = 3.6228, MSE-V = 3.3113, PSNR-Y = 37.9785, PSNR-U = 42.5403, PSNR-V = 42.9308

(e) MSE-Y = 14.0693, MSE-U = 4.0741, MSE-V = 4.4404, PSNR-Y = 36.6481, PSNR-U = 42.0304, PSNR-V = 41.6566

(f) MSE-Y = 14.5953, MSE-U = 4.1377, MSE-V = 4.6053, PSNR-Y = 36.4887, PSNR-U = 41.9632, PSNR-V = 41.4982

(g) MSE-Y = 14.6155, MSE-U = 4.1349, MSE-V = 4.5502, PSNR-Y = 36.4827, PSNR-U = 41.9661, PSNR-V = 41.5505

(h) MSE-Y = 15.0761, MSE-U = 4.2812, MSE-V = 4.6444, PSNR-Y = 36.3479, PSNR-U = 41.8151, PSNR-V = 41.4615

Figure 12: Compression of the tenth frame of `BasketballDrive` using (a),(c),(e) the default and (b),(d),(f) the modified versions of the HEVC software for QP = 32, and AI, RA, LD-B, and LD-P coding configurations, respectively.

[8] J. Bae and H. Yoo, "Analysis of color transforms for lossless frame memory compression," *International Journal of Applied Engineering Research*, vol. 12, no. 24, pp. 15 664–15 667, 2017. 1

[9] D. Thomakos, "Smoothing non-stationary time series using the discrete cosine transform," *Journal of Systems Science and Complexity*, vol. 29, no. 2, pp. 382–404, 2016. 1

[10] J. Zeng, G. Cheung, Y.-H. Chao, I. Blanes, J. Serra-Sagristá, and A. Ortega, "Hyperspectral image coding using graph wavelets," in *Proc. IEEE International Conference on Image Processing (ICIP)*, 2017. 1

[11] R. E. Blahut, *Fast algorithms for signal processing*. Cambridge University Press, 2010. 1, 3, 6

[12] N. Ahmed, T. Natarajan, and K. R. Rao, "Discrete cosine transform," *IEEE Transactions on Computers*, vol. C-23, no. 1, pp. 90–93, Jan. 1974. 1, 6

[13] R. J. Clarke, "Relation between the Karhunen-Loève and cosine transforms," *IEEE Proceedings F Communications, Radar and Signal Processing*, vol. 128, no. 6, pp. 359–360, Nov. 1981. 1

[14] R. J. Cintra, F. M. Bayer, and C. J. Tablada, "Low-complexity 8-point DCT approximations based on integer functions," *Signal Processing*, 2014. 1, 2, 4, 6, 7, 8

[15] R. C. Gonzalez and R. E. Woods, *Digital image processing*, 3rd ed. Upper Saddle River, NJ, USA: Prentice-Hall, Inc., 2006. 1

[16] G. K. Wallace, "The JPEG still picture compression standard," *IEEE Transactions on Consumer Electronics*, vol. 38, no. 1, pp. xviii–xxxiv, February 1992. 1, 7

[17] A. Puri, "Video coding using the H.264/MPEG-4 AVC compression standard," *Signal Processing: Image Communication*, vol. 19, 2004. 1

[18] D. J. Le Gall, "The MPEG video compression algorithm," *Signal Processing: Image Communication*, vol. 4, no. 2, pp. 129–140, 1992. 1

[19] International Telecommunication Union, "ITU-T recommendation H.261 version 1: Video codec for audiovisual services at $p \times 64$ kbits," ITU-T, Tech. Rep., 1990. 1

[20] ——, "ITU-T recommendation H.263 version 1: Video coding for low bit rate communication," ITU-T, Tech. Rep., 1995. 1

[21] A. Luthra, G. J. Sullivan, and T. Wiegand, "Introduction to the special issue on the H.264/AVC video coding standard," *IEEE Transactions on Circuits and Systems for Video Technology*, vol. 13, no. 7, pp. 557–559, Jul. 2003. 1

[22] M. T. Pourazad, C. Doutre, M. Azimi, and P. Nasiopoulos, "HEVC: The new gold standard for video compression: How does HEVC compare with H.264/AVC?" *IEEE Consumer Electronics Magazine*, vol. 1, no. 3, pp. 36–46, Jul. 2012. 1, 9

[23] C. Loeffler, A. Ligtenberg, and G. Moschytz, "Practical fast 1D DCT algorithms with 11 multiplications," in *Proceedings of the International Conference on Acoustics, Speech, and Signal Processing*, May 1989, pp. 988–991. 1, 2, 7

[24] U. Sadhvi Potluri, A. Madanayake, R. J. Cintra, F. M. Bayer, S. Kulasekera, and A. Edirisuriya, "Improved 8-point approximate DCT for image and video compression requiring only 14 additions," *Circuits and Systems I: Regular Papers, IEEE Transactions on*, vol. 61, no. 6, pp. 1727–1740, 2014. 1, 7

[25] V. A. Coutinho, R. J. Cintra, F. M. Bayer, S. Kulasekera, and A. Madanayake, "A multiplierless pruned DCT-like transformation for image and video compression that requires ten additions only," *Journal of Real-Time Image Processing*, pp. 1–9, 2015. 1, 9

[26] F. M. Bayer, R. J. Cintra, A. Edirisuriya, and A. Madanayake, "A digital hardware fast algorithm and FPGA-based prototype for a novel 16-point approximate DCT for image compression applications," *Measurement Science and Technology*, vol. 23, no. 8, p. 114010, November 2012. 1

[27] F. M. Bayer and R. J. Cintra, "Image compression via a fast DCT approximation," *IEEE Latin America Transactions*, vol. 8, no. 6, pp. 708–713, Dec. 2010. 1, 2, 4, 6, 7

[28] W. Yuan, P. Hao, and C. Xu, "Matrix factorization for fast DCT algorithms," in *IEEE International Conference on Acoustic, Speech, Signal Processing (ICASSP)*, vol. 3, May 2006, pp. 948–951. 2

[29] Y. Arai, T. Agui, and M. Nakajima, "A fast DCT-SQ scheme for images," *Transactions of the IEICE*, vol. E-71, no. 11, pp. 1095–1097, Nov. 1988. 2

[30] W. H. Chen, C. Smith, and S. Fralick, "A fast computational algorithm for the discrete cosine transform," *IEEE Transactions on Communications*, vol. 25, no. 9, pp. 1004–1009, September 1977. 2, 11

[31] E. Feig and S. Winograd, "Fast algorithms for the discrete cosine transform," *IEEE Transactions on Signal Processing*, vol. 40, no. 9, pp. 2174–2193, September 1992. 2

[32] B. G. Lee, "A new algorithm for computing the discrete cosine transform," *IEEE Transactions on Acoustics, Speech and Signal Processing*, vol. ASSP-32, pp. 1243–1245, Dec. 1984. 2

[33] H. S. Hou, "A fast recursive algorithm for computing the discrete cosine transform," *IEEE Transactions on Acoustic, Signal, and Speech Processing*, vol. 6, no. 10, pp. 1455–1461, October 1987. 2, 6

[34] M. T. Heideman and C. S. Burrus, *Multiplicative complexity, convolution, and the DFT*, ser. Signal Processing and Digital Filtering. Springer-Verlag, 1988. 2

[35] J. Liang and T. D. Tran, "Fast multiplierless approximation of the DCT with the lifting scheme," *IEEE Transactions on Signal Processing*, vol. 49, pp. 3032–3044, December 2001. 2, 5

[36] M. Masera, M. Martina, and G. Masera, "Odd type DCT/DST for video coding: Relationships and low-complexity implementations," 2017. 2

[37] Z. Wang, "Combined DCT and companding for PAPR reduction in OFDM signals." *J. Signal and Information Processing*, vol. 2, no. 2, pp. 100–104, 2011. 2

[38] F. S. Snigdha, D. Sengupta, J. Hu, and S. S. Sapatnekar, "Optimal design of JPEG hardware under the approximate computing paradigm," in *Proceedings of the 53rd Annual Design Automation Conference*. ACM, 2016, p. 106. 2

[39] T. Suzuki and M. Ikehara, "Integer DCT based on direct-lifting of DCT-IDCT for lossless-to-lossy image coding," *IEEE Transactions on Image Processing*, vol. 19, no. 11, pp. 2958–2965, Nov. 2010. 2

[40] C.-K. Fong and W.-K. Cham, "LLM integer cosine transform and its fast algorithm," *IEEE Transactions on Circuits and Systems for Video Technology*, vol. 22, no. 6, pp. 844–854, 2012. 2

[41] K. Choi, S. Lee, and E. S. Jang, "Zero coefficient-aware IDCT algorithm for fast video decoding," *IEEE Transactions on Consumer Electronics*, vol. 56, no. 3, 2010. 2

[42] M. Masera, M. Martina, and G. Masera, "Adaptive approximated dct architectures for hevc," *IEEE Transactions on Circuits and Systems for Video Technology*, vol. 27, no. 12, pp. 2714–2725, 2017. 2

[43] J.-S. Park, W.-J. Nam, S.-M. Han, and S.-S. Lee, "2-D large inverse transform (16× 16, 32× 32) for HEVC (high efficiency video coding)," *JSTS: Journal of Semiconductor Technology and Science*, vol. 12, no. 2, pp. 203–211, 2012. 2

[44] X. Xu, J. Li, X. Huang, M. Dalla Mura, and A. Plaza, "Multiple morphological component analysis based decomposition for remote sensing image classification," *IEEE Transactions on Geoscience and Remote Sensing*, vol. 54, no. 5, pp. 3083–3102, 2016. 2

[45] N. J. Higham, "Computing the polar decomposition—with applications," *SIAM Journal on Scientific and Statistical Computing*, vol. 7, no. 4, pp. 1160–1174, Oct. 1986. 2, 3, 4

[46] R. J. Cintra and F. M. Bayer, "A DCT approximation for image compression," *IEEE Signal Processing Letters*, vol. 18, no. 10, pp. 579–582, Oct. 2011. 2, 3, 5, 7

[47] R. J. Cintra, "An integer approximation method for discrete sinusoidal transforms," *Journal of Circuits, Systems, and Signal Processing*, vol. 30, no. 6, pp. 1481–1501, December 2011. 2, 3, 4

[48] F. M. Bayer and R. J. Cintra, "DCT-like transform for image compression requires 14 additions only," *Electronics Letters*, vol. 48, no. 15, pp. 919–921, Jul. 2012. 2, 5, 6, 7

[49] N. J. Higham, "Computing real square roots of a real matrix," *Linear Algebra and its Applications*, vol. 88–89, pp. 405–430, April 1987. 2

[50] G. A. F. Seber, *A Matrix Handbook for Statisticians*, ser. Wiley Series in Probability and Mathematical Statistics. Wiley, 2008. 2, 11

[51] T. I. Haweel, "A new square wave transform based on the DCT," *Signal Processing*, vol. 82, pp. 2309–2319, November 2001. 2, 5, 6, 7

[52] S. Bouguezel, M. O. Ahmad, and M. N. S. Swamy, "Low-complexity 8×8 transform for image compression," *Electronics Letters*, vol. 44, no. 21, pp. 1249–1250, Sep. 2008. 2, 6, 7

[53] ——, "Low-complexity 8×8 transform for image compression," *Electronics Letters*, vol. 44, no. 21, pp. 1249–1250, 2008. 2, 6, 7

[54] ——, “A fast 8×8 transform for image compression,” in *2009 International Conference on Microelectronics (ICM)*, Dec. 2009, pp. 74–77. 2, 6, 7

[55] ——, “A low-complexity parametric transform for image compression,” in *Proceedings of the 2011 IEEE International Symposium on Circuits and Systems*, May 2011. 2, 6, 7

[56] ——, “Binary discrete cosine and Hartley transforms,” *IEEE Transactions on Circuits and Systems I: Regular Papers*, vol. 60, no. 4, pp. 989–1002, April 2013. 2, 6, 7

[57] K. Lengwehasatit and A. Ortega, “Scalable variable complexity approximate forward DCT,” *IEEE Transactions on Circuits and Systems for Video Technology*, vol. 14, no. 11, pp. 1236–1248, Nov. 2004. 2, 6, 7, 8, 12

[58] R. K. Senapati, U. C. Pati, and K. K. Mahapatra, “A low complexity orthogonal 8×8 transform matrix for fast image compression,” *Proceeding of the Annual IEEE India Conference (INDICON), Kolkata, India*, pp. 1–4, 2010. 2

[59] W. K. Cham, “Development of integer cosine transforms by the principle of dyadic symmetry,” in *IEE Proceedings I Communications, Speech and Vision*, vol. 136, no. 4, August 1989, pp. 276–282. 2

[60] T. Cormen, C. Leiserson, R. Rivest, and C. Stein, *Introduction To Algorithms*. MIT Press, 2001, ch. 16. 3, 4, 6

[61] C. J. Tablada, F. M. Bayer, and R. J. Cintra, “A class of DCT approximations based on the Feig–Winograd algorithm,” *Signal Processing*, vol. 113, pp. 38–51, 2015. 3, 7, 9

[62] G. Strang, *Linear Algebra and Its Applications*. Brooks Cole, Feb. 1988. 3

[63] D. Salomon, G. Motta, and D. Bryant, *Data Compression: The Complete Reference*, ser. Molecular biology intelligence unit. Springer, 2007. 4, 7

[64] N. J. Higham and R. S. Schreiber, “Fast polar decomposition of an arbitrary matrix,” Ithaca, NY, USA, Tech. Rep., October 1988. 4

[65] Z. Wang and A. C. Bovik, “Mean squared error: Love it or leave it? A new look at signal fidelity measures,” *IEEE Signal Processing Magazine*, vol. 26, no. 1, pp. 98–117, Jan. 2009. 5, 7

[66] V. K. Goyal, “Theoretical foundations of transform coding,” *IEEE Signal Processing Magazine*, vol. 18, no. 5, pp. 9–21, September 2001. 5

[67] J. Katto and Y. Yasuda, “Performance evaluation of subband coding and optimization of its filter coefficients,” *Journal of Visual Communication and Image Representation*, vol. 2, no. 4, pp. 303–313, December 1991. 5

[68] K. Mardia and P. Jupp, *Directional Statistics*, ser. Wiley Series in Probability and Statistics. Wiley, 2009. 5

[69] S. Jammalamadaka and A. Sengupta, *Topics in Circular Statistics*, ser. Series on multivariate analysis. World Scientific, 2001. 5

[70] D. S. Watkins, *Fundamentals of Matrix Computations*, ser. Pure and Applied Mathematics: A Wiley Series of Texts, Monographs and Tracts. Wiley, 2004. 5

[71] R. P. Mahan, *Circular Statistical Methods: Applications in Spatial and Temporal Performance Analysis*, ser. Special report. U.S. Army Research Institute for the Behavioral and Social Sciences, 1991. 5

[72] J.-R. Ohm, G. J. Sullivan, H. Schwarz, T. K. Tan, and T. Wiegand, “Comparison of the coding efficiency of video coding standards - including High Efficiency Video Coding (HEVC),” *IEEE Transactions on Circuits and Systems for Video Technology*, vol. 22, no. 12, pp. 1669–1684, Dec. 2012. 5, 6, 7, 9, 12

[73] J. Han, Y. Xu, and D. Mukherjee, “A butterfly structured design of the hybrid transform coding scheme,” in *Picture Coding Symposium (PCS), 2013*. IEEE, 2013, pp. 17–20. 6

[74] P. Yip and K. Rao, “The decimation-in-frequency algorithms for a family of discrete sine and cosine transforms,” *Circuits, Systems and Signal Processing*, vol. 7, no. 1, pp. 3–19, 1988. 6

[75] I.-M. Pao and M.-T. Sun, “Approximation of calculations for forward discrete cosine transform,” *IEEE Transactions on Circuits and Systems for Video Technology*, vol. 8, no. 3, pp. 264–268, Jun. 1998. 7

[76] (2017) USC-SIPI Image Database. University of Southern California. [Online]. Available: http://sipi.usc.edu/database/ 7

[77] Z. Wang, A. C. Bovik, H. R. Sheikh, and E. P. Simoncelli, “Image quality assessment: from error visibility to structural similarity,” *IEEE Transactions on Image Processing*, vol. 13, no. 4, pp. 600–612, Apr. 2004. 7

[78] N. J. Higham, *Functions of Matrices: Theory and Computation*, ser. SIAM e-books. Society for Industrial and Applied Mathematics (SIAM, 3600 Market Street, Floor 6, Philadelphia, PA 19104), 2008. 7

[79] R. K. W. Chan and M.-C. Lee, “Multiplierless fast DCT algorithms with minimal approximation errors,” in *International Conference on Pattern Recognition*, vol. 3. Los Alamitos, CA, USA: IEEE Computer Society, 2006, pp. 921–925. 9

[80] V. Dimitrov, G. Jullien, and W. Miller, “A new DCT algorithm based on encoding algebraic integers,” in *Proceedings of the 1998 IEEE International Conference on Acoustics, Speech and Signal Processing, 1998.*, vol. 3, May 1998, pp. 1377–1380 vol.3. 9

[81] Joint Collaborative Team on Video Coding (JCT-VC), “HEVC reference software documentation,” 2013, Fraunhofer Heinrich Hertz Institute. [Online]. Available: https://hevc.hhi.fraunhofer.de/ 9

[82] G. J. Sullivan, J.-R. Ohm, W.-J. Han, and T. Wiegand, “Overview of the high efficiency video coding (HEVC) standard,” *IEEE Trans. Circuits Syst. Video Technol.*, vol. 22, no. 12, pp. 1649–1668, Dec. 2012. 9

[83] M. Jridi, A. Alfalou, and P. K. Meher, “A generalized algorithm and reconfigurable architecture for efficient and scalable orthogonal approximation of DCT,” *IEEE Trans. Circuits Syst. I*, vol. 62, no. 2, pp. 449–457, 2015. 11, 12

[84] P. K. Meher, S. Y. Park, B. K. Mohanty, K. S. Lim, and C. Yeo, “Efficient integer DCT architectures for HEVC,” *IEEE Transactions on Circuits and Systems for Video Technology*, vol. 24, no. 1, pp. 168–178, Jan 2014. 11, 12

[85] F. Bossen, “Common test conditions and software reference configurations,” San Jose, CA, USA, Feb 2013, document JCT-VC L1100. 11, 12

[86] G. Bjøntegaard, “Calculation of average PSNR differences between RD-curves,” in *13th VCEG Meeting*, Austin, TX, USA, Apr 2001, document VCEG-M33. 12

[87] P. Hanhart and T. Ebrahimi, “Calculation of average coding efficiency based on subjective quality scores,” *Journal of Visual Communication and Image Representation*, vol. 25, no. 3, pp. 555 – 564, 2014, qoE in 2D/3D Video Systems. 12